Authors Response

Anomalies in the Carbonate System of Red Sea Coastal Habitats

Kimberlee Baldry, Vincent Saderne, Daniel C. McCorkle, James H. Churchill, Susana Agusti and Carlos M. Duarte

We thank the editors for inviting us to resubmit our article, and the reviewers who took the time to read and comment on it. Within this document we have included:

List of relevant major changes

- Added in data from Steiner et al. (2018). Re-running results, reproducing figures and amending results.
- Created Figure 3 to reassess long-term trends in TA
- Moving a figure to the supplementary information (Figure S2)
- Adding in discussion around the long-term trends

Point-by -point response to Reviewer 1

Author response to Reviewer Comment 1: Zvi Steiner

Key:

- Review comment is in **bold**
- Author response is in normal text
- Changes made are in *italics*

We thank Dr. Zvi Steiner for their contribution to the review process of this paper. We have considered the reviewers comments carefully and incorporated their feedback in the below dialogue.

Baldry et al., report analyses of alkalinity and dissolved inorganic carbon along the main axis of the Red Sea and into some of the region's coastal ecosystem. These measurements are used to assess the magnitude of changes in total alkalinity and dissolved inorganic carbon in the various ecosystems of the Red Sea. The Red Sea has an exceptionally long stretch of tropical coastal habitats that are under increasing pressure globally. The unique oceanographic conditions of this region, e.g. relatively simple flow regime, high salinity and high temperatures turn the Red Sea into a very relevant site for studying how changes in different environmental variables affect coral reefs, mangroves and seagrass meadows. It is also a region that was historically very poorly represented in oceanographic studies.

This paper provides an important dataset which is an essential addition to the data currently available in the scientific literature. I think that the discussion of this data could be made substantially stronger if it will be better tied to previous publications and used to explain changes that were observed in the carbonate system of the Red Sea. As noted by the authors, there has be a large increase in the total alkalinity of the Red Sea surface waters in recent years (Steiner et al., 2018).

Previous publications on this topic were limited in their ability to assess if this change was only due to changes in coral calcification and ecology or there has been a shift in other ecosystems as well, and whether or not these correlate with each other. The authors chose to ignore half of their dataset and focus exclusively on the older samples but I think that comparisons between old and new trends of ecosystem specific rTA and rDIC could be valuable.

Together with comparison with past data regarding the change in DIC and total alkalinity of the central Red Sea axis, this can potentially provide a test for the various hypotheses previously suggested for the cause of the reduction in Red Sea calcification rates.

We thank the reviewer for the positive comments and the guidance provided. We focused our study in offshore Red Sea data published in the literature that is less than 10 years old, as well as new offshore data collected within the scope of the study to train our offshore model and calculate ecosystem specific rTA and rDIC. We noted a trend in TA and DIC in our offshore data compared to old cruises, which support the findings of Steiner et al. 2018. We are taking the reviewers comments on board and adding an extra subplot to Figure 4 to confirm the differences between old and new data with an independent dataset from 1982. This data will be made openly available via PANGAE upon acceptance of the manuscript.

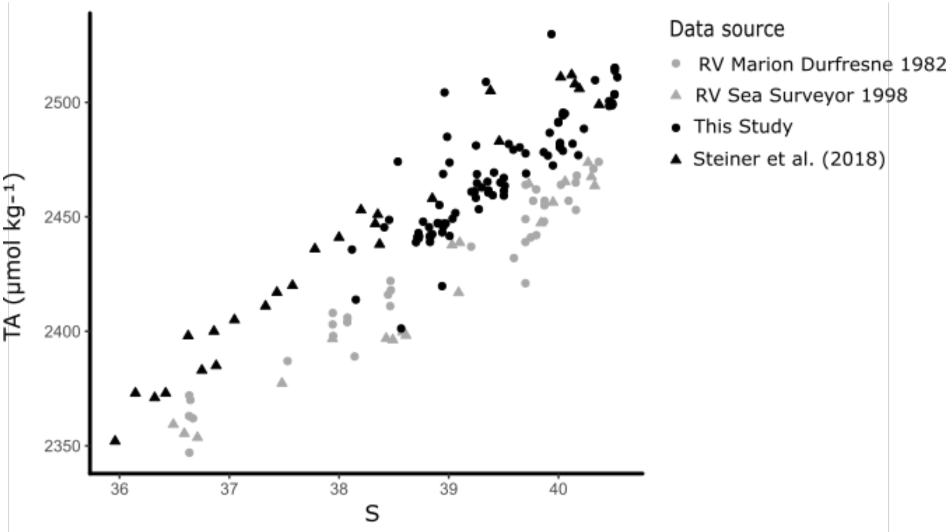

We also note that we did not include data reported in Steiner et al. (2018) in our published dataset. We have now added this data to our analysis, increasing the transition water dataset from 71 to 72 and the offshore dataset from 92 to 101. The inclusion has not changed the results or main findings of the paper substantially, and we will be happy to work this into our revised manuscript. A revised Section 3.1 and Table S2 is shown below to illustrate the minor changes the adding in the Steiner et al. (2018) data has to our model.

3.1 The Red Sea offshore end-member

The offshore carbonate system of the Red Sea was characterized along the south-north central axis. Offshore waters exhibited significant and strong (high r^2) linear increases in S, TA and DIC along the central south-north axis of the Red Sea as indicated by respective regression analysis with D (Figure 3, Table S3). TA and DIC were normalized to a salinity of 35 (nTA and nDIC), and both exhibited significant and weak (low r^2) linear decreases along the central south-north axis of the Red Sea (Figure 4). However, winter nDIC values appear to deviate from this linear relationship. The nTA and nDIC co-varied along this axis in an average ratio of 0.87 (SE= 0.07, r^2 = 0.60, F = 147.7, p<0.001) nTA to 1 nDIC (Figure 4c). A significant and weak (low r^2) linear decrease was found for T against D, that displayed clear seasonal dependencies between summer and winter/spring temperatures (Figure 3). A significant and weak (low r^2) increase in pH, a significant and weak (low r^2) decrease in pCO_2, and no significant linear relationship in Ω_A, against D were also observed.

In defining the offshore end-member for implementation in the single-end-member mixing model, offshore observations not representative of the expected linear relationships in the surface offshore Red Sea were removed. These were identified as eleven outlying offshore observations exhibiting a Cook's distance greater than five times the mean in at least one of the three linear models of D, against S, TA and DIC (Figure 1; Cook and Weisberg, 1997). Linear models were then re-fit with the remaining offshore observations (n = 104) to yield Equations 3-5, to be substituted into Equations 1-2 to complete the single-end-member mixing model (Figure 3).

Equation 3: $S_O = 0.00157*D + 37.47$

Equation 4: $TA_O = 0.0510*D + 2407$

Equation 5: $DIC_O = 0.0437*D + 2029$

*To approximate the error of the single-end-member mixing model, 99% prediction intervals (99% P.I. = mean ± 2.576*sd) were calculated by applying the single-end-member mixing model to offshore observations to yield rTA, rDIC, rpCO*$_2$*, rpH and r*Ω_{Ar} *(Table S2). These 99% P.I represent a cumulative error due to the natural variations of* S_O, TA_O *and* DIC_O*, along with the error propagation associated with the calculations of other carbon parameters. Two offshore observations used in defining the offshore end-member fell outside the 99% P.I., both exhibiting high TA, and one exhibiting high DIC.*

Table S2: *Defining statistics of the normal error for residual carbon variable estimates, as calculated from offshore observations*

	Residual mean	Residual standard deviation	Lower 99% P.I. bound+	Upper 99% P.I. bound++	% offshore observations outside the 99% P.I. (excluding/including outliers)
rTA (µmol/kg)	0	16.79	-43.25	43.25	1.1/5.9
rDIC (µmol/kg)	0	23.33	-60.09	60.09	2.2/5.9
rpH	-5×10^{-4}	2.69×10^{-2}	-6.97×10^{-2}	6.87×10^{-2}	4.3/6.9
rpCO$_2$ (µatm)	0.10	30.20	-77.69	77.90	4.3/7.9
rΩ_{Ar}	0.0006	0.1879	-0.4833	0.4845	4.3/6.9

Whereas, the long-term trends observed in the Red Sea are not the focus of this study, we do believe that adding an element in the discussion using our new results to provide some insights onto the long-term changes noted by Steiner et al. (2018), will add value to the paper, as suggested by the reviewer. We have, therefore, added the following paragraph in the discussion section:

"The results reported here can offer explanation to the decadal changes in calcification rates in the Red Sea reported by Steiner et al. (2018), which are also supported by inspection of the data compiled

here (Figure 4a). Steiner et al. (2018), reported a 26 ± 16% decline in total $CaCO_3$ deposition rate along the basin between 1998 and 2018, concentrated in the southern Red Sea, suggesting that coral reefs in the southern Red Sea are under stress. Indeed, warming of the Red Sea, which has been faster than the global average (Chaidez et al. 2017), has been reported to reduce coral growth rates (Cantin et al. 2010), and massive bleaching of Red Sea corals south of 20ºN in the summer of 2015 (Hughes et al. 2018, Osman et al. 2018), and replacement by algal turf, may have reduced carbonate deposition rates in the southern Red Sea further. Our analysis suggests additional contributions to decline carbonate deposition in the Red Sea. In particular, mangrove habitats are characterized here as important sites of carbonate dissolution. Hence, the 13% increase in mangrove forests in the Red Sea over the past 30 years (Almahasheer et al. 2016), is expected to have resulted in increased rates of carbonate dissolution basin-wide."

Additional references.

Cantin, N. E., Cohen, A. L., Karnauskas, K. B., Tarrant, A. M. & McCorkle, D. C. Ocean warming slows coral growth in the central Red Sea. Science 329, 322–325 (2010).

Osman, E.O., Smith, D.J., Ziegler, M., Kürten, B., Conrad, C., El-Haddad, K.M., Voolstra, C.R. and Suggett, D.J., 2018. Thermal refugia against coral bleaching throughout the northern Red Sea. Global change biology, 24(2), pp.e474-e484.

Hughes, T. P. et al. Spatial and temporal patterns of mass bleaching of corals in the Anthropocene. Science 359, 80–83 (2018).

Chaidez, V., Dreano, D., Agusti, S., Duarte, C.M. and Hoteit, I., 2017. Decadal trends in Red Sea maximum surface temperature. Scientific reports, 7(1), p.8144.

A few specific comments:

Please refrain from using the shortcuts OCP and D. They are not intuitive and had me going back to check their meaning several times.

Noted. We will remove the acronym OCP. However, we need to retain the acronym D, as it is a key model parameter that we define in the methods and in Figure 2. We have edited the methodology to make what D more obvious to the reader by defining it first in the single end-member model.

OCP replaced with other carbon parameter. First paragraph of 2.4 now reads:

"A single-end-member mixing model was used to model conservative TA (cTA) and conservative DIC (cDIC) for coastal observations. First, the perpendicular distance of a point along the central axis of the Red Sea in km (D) was calculated for each observation. This was done using the "alongTrackDistance" function (default settings) in the R package "geosphere" (Hijmans, 2017) with the reference point 12.7737°N 43.2618°E to represent D = 0 and the reference point 28.2827°N 34.0694°E to define position of the central south-north axis. The single-end-member model was then implemented by 1) describing the linear variations of S, TA and DIC with D, so that predictions of offshore S (S_O), offshore TA (TA_O) and offshore DIC (DIC_O) can be made from D corresponding to coastal observations, and then 2) calculating cTA and cDIC for coastal observations according to Equations 1-2, which predict the simple dilution and concentration (SDC) effects of coastal evaporation (Figure 2)."

Caption edited from "…….. O_i represents a location in the offshore end-member lying along the central axis at distance D_i,….." to "…….. O_i represents a location in the offshore end-member lying along flow axis 1 (the central axis) at distance D_i,….."

Fig. 3: please indicate in the figure legend if these are surface waters only.

Noted.

"Observations of S, T and carbon variables in the offshore end-member (left)" changed to "Observations of S, T and carbon variables in the surface offshore end-member (left)"

Fig. 6: I don't understand from the legend what A, B, C, AB etc. stand for. It needs to be explained in the paper, not in the appendix.

Noted.

Figure 7 caption changed from "Grouping letters indicate the results of post-hoc bootstrapped t-tests, summarized from statistics presented in Table S5. If tests showed significant similarities at the 0.05 significance level with another habitat across a variable they were assigned the same letter." to "Grouping letters (A-D) assigned above boxplots indicate the results of post-hoc bootstrapped t-tests, summarized from statistics presented in Table S5. If tests showed significant similarities at the 0.05 significance level with another habitat across a variable they were assigned the same letter."

Fig. 7: From which year is the data presented here?

2016/2017.

Figure 7 x-label changed to month/year (below). Mm/dd is a mistake. Thank you!

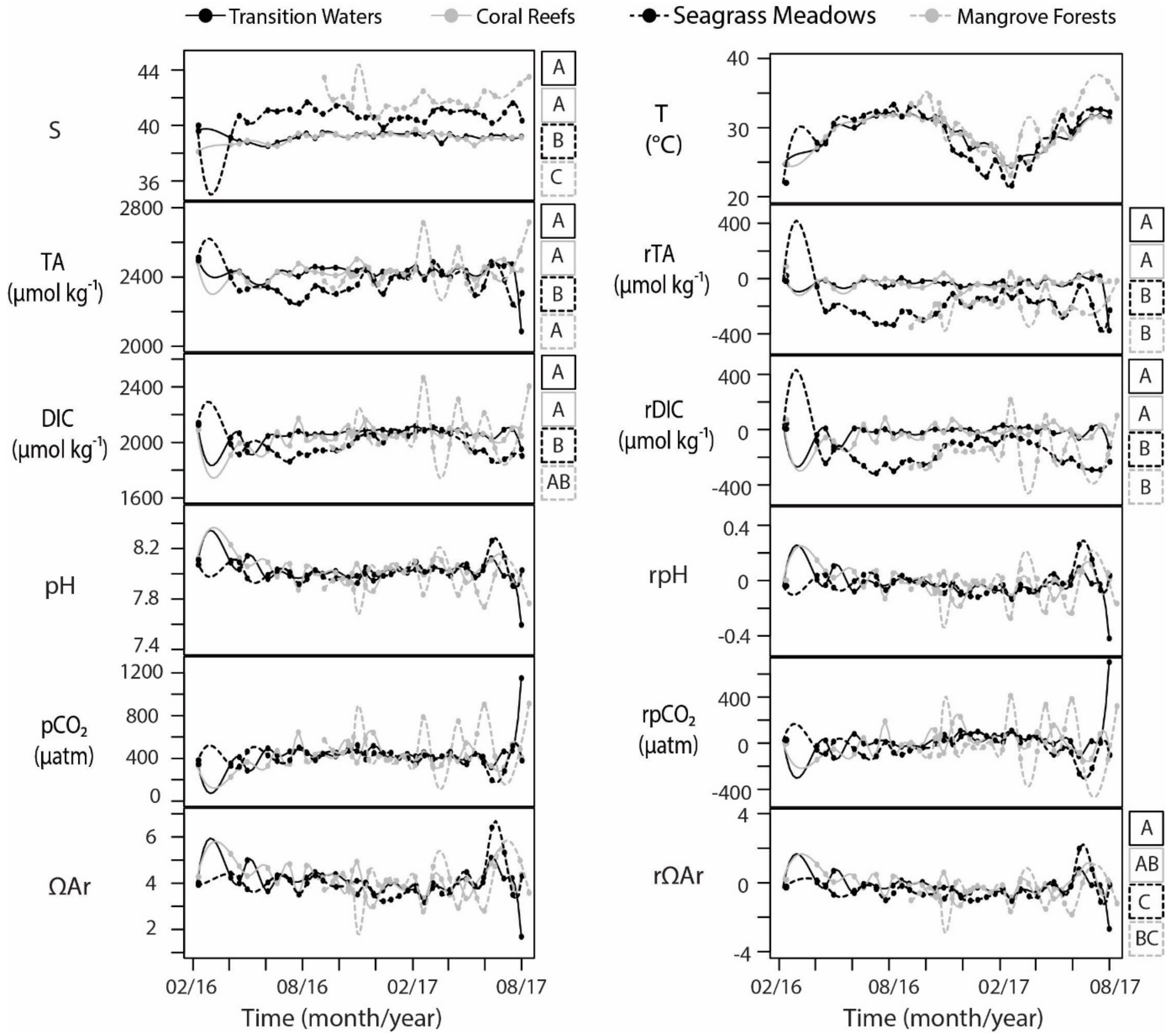

Transition Waters
Coral Reefs
Seagrass Meadows
Mangrove Forests
S
T (°C)
TA (µmol kg-1)
rTA (µmol kg-1)
DIC (µmol kg-1)
rDIC (µmol kg-1)
pH
rpH
pCO2 (µatm)
rpCO2 (µatm)
ΩAr
rΩAr
Time (month/year)
Time (month/year)
02/16
08/16
02/17
08/17

Point-by -point response to Reviewer 2

Author Response to Reviewer Comment 2: Anonymous Reviewer 2

Key:

- Review comment is in **bold**
- Author response is in normal text
- Changes made are in *italics*

We thank Reviewer 2 for their contribution to the review process of this paper. We have considered the reviewers comments carefully and incorporated their feedback in the below dialogue.

General comments: In this paper, Baldry et al. combine carbon measurements from the open ocean and east coastal areas in the Red Sea to model ecosystem-driven changes on the carbon system of coral reefs, mangrove forest, and seagrass meadows. In this region, oceanographic studies in general as well as carbon and ecosystem studies are heavily underrepresented, despite its extreme conditions regarding hydrography and vulnerable ecosystems. The paper by Baldry et al. represent an important contribution to the biogeochemical research from the Red Sea, and by using novel data, historical data, and a model tool, they increase our knowledge about driving forces for coastal ecosystems.

More specific comments:

The word "trend" is used but the word refers to change over time, and you do not use the word this way. As I understand, you simply mean linear relationship between e.g. offshore salinity and distance from a point in the southern Red Sea, or alkalinity and the mentioned distance.

This is correct. We are describing linear relationships and not trends with time

The terms "trends" and "linear trends" have been replaced with "linear relationships", except when used in the context of seasonal changes. Here, the term "seasonal trend" has been changed to "seasonal dependency"

Every now and then you put up statements and explain them later in the manuscript, e.g. P2, L22 about linear trends, P4, L18 where you introduce D without explaining it until later in the text. I encourage you to gather the statement and explanation, to make the reading easier.

We agree these issues need be addressed. We have altered the identified problems as outlined in the specific comments, in particular introducing and explaining D. The f*irst paragraph of 2.4(now 2.5) now reads:*

"A single-end-member mixing model was used to model conservative TA (cTA) and conservative DIC (cDIC) for coastal observations. First, the distance of a point along the central axis of the Red Sea in km (D) was calculated for each observation. This was done using the "alongTrackDistance" function (default settings) in the R package "geosphere" (Hijmans, 2017) with the reference point 12.7737°N 43.2618°E to represent D = 0 and the reference point 28.2827°N 34.0694°E to define position of the central south-north axis. The single-end-member model was then implemented by 1) describing the linear variations of offshore S, TA and DIC with D, so that predictions of offshore S (S_O), offshore TA (TA_O) and offshore DIC (DIC_O) can be made from the value of D corresponding to coastal observations, and then 2) calculating cTA and cDIC for observations according to Equations 1-2, which predict the simple dilution and concentration (SDC) effects of evaporation (Figure 2)."

You refer to numerous interesting papers, please include a separation between ";" and the following author name. This comment is valid for the whole paper. E.g. L 28: (Bauer et al., 2013; Camp et al., 2016; Cyronak et al., 2018; Gattuso et al., 1998; Guannel et al., 2016; Unsworth et al., 2012) – here I have added space.

Noted.

A space has been added between ";" and the following author name.

You discuss several limitations with the single-end-member model, but you actually did choose this model. Please add an argument stating why, despite all its limitations, you made this decision.

Noted.

We have adjusted section 2.6 as follows:

2.6 Model Assumptions and Limitations

The single-end-member mixing model assumes simple two-dimensional circulation in a region that exhibits more complex flow. The modelled flow follows a south-north trajectory along the central axis of the Red Sea, with perpendicular coastal flushing from offshore waters located at similar distances along the central axis (Figure 2). This allows changes in the carbonate chemistry of offshore waters, due to both conservative and non-conservative processes, and conservative coastal evaporation to be modelled.

It is well known that this is not the case and the Red Sea has a complex surface flow displaying multiple dynamic eddies along its length (Sofianos and Johns, 2003; Zhan et al., 2014). Depending on the direction of flow, these eddies promote coastal flushing from offshore waters originating further north or further south along the central axis of the Red Sea, mixing in a way the simple single-end-member mixing model cannot capture. Other limitations of the simple single-end-member model include its inability to account for coastal upwelling along the continental shelf, variable mixing of Gulf of Aden waters with Red Sea offshore waters and changes in basin-scale evaporation and calcification which have been documented in previous studies (Anderson and Dyrssen, 1994; Churchill et al., 2014; Krumgalz et al., 1990; Papaud and Poisson, 1986; Steiner et al., 2018).

These limitations cannot be addressed within the present study and require a sustained observational effort to address knowledge gaps in the carbon chemistry of the Red Sea, combined with more complex circulation models. Complex circulation models could capture some large-scale variance in circulation, but they are costly simulations that may still produce questionable results due to the unresolved coastal bathymetry of the Red Sea. Instead, we use the 99% P.I. of offshore carbonate chemistry residuals as a bound of model error, and to capture deviations from modelled carbonate chemistry due to variations in circulation.

You use the words strong or weak linear increase when you actually mean high or low r2. Just be aware that strong/weak linear increase might also be understood as a line with high or low slope.

We have attempted to make the association between strong/weak to r2 in the text by referencing to r2 values in parentheses more often. We have also edited section "2.7 Statistical tests" to read

"All statistical tests were performed using R software (R core team, 2017) with a 95% confidence level. Least squares regression analysis was used to calculate linear relationships with D for S, temperature and carbonate variables, thus determining how S, temperature and carbonate variables vary along the central axis from south to north. Least squares regression analysis was also used to calculate relationships between rTA and rDIC. The square of Pearson's correlation coefficient (r^2) of linear relationships was used to evaluate the strength of the relationships."

Detailed comments:

P1 L16: you introduce the word "trend", which refer to change over time. But this is not what you mean, right? Rather use "linear relationship"

Addressed above

P2 L11: I suggest a more direct language: As such, these non-conservative changes can be measured as anomalies from the carbonate system which has experienced conservative mixing.

Thank you.

This suggestion has been taken throughout the paper, and the use of the term "norm" removed from the text throughout.

L22: You state "The linear trend in offshore carbonate system concentrations..." without explaining or showing what you mean by this. Again, I suspect that you mean simply linear relationship and not trend.

Addressed above.

L23: suggest to not use the word "norm" but only "expected conservative behaviour"

Changed.

"norm" replaced with "expected conservative behaviour"

P3 L27: second last word: switch "a" with "an"

Changed.

"a" replaced with "an"

L27: please add if this method also use non-linear curve fitting

Changed.

"and TA was measured by open-cell titration with 0.1 M hydrochloric acid using a Mettler Toledo T50 Autotitrator equipped with an InMotion Pro Autosampler" to "and TA was measured by open-cell titration with 0.1 M hydrochloric acid using a Mettler Toledo T50 Autotitrator equipped with an InMotion Pro Autosampler using non-linear curve fitting to determine an equivalence point"

L29: add full address of Dr. A. Dickson the first time he is mentioned

Addressed

"Dr. A. Dickson" changed to "Dr. Andrew Dickson (Scripps Institution of Oceanography)" on first occurrence

L35: which type of CTD is used

We cannot address this point; we do not know the make and model of the ship's CTD. We do not see this as a critical lack.**L36: I guess you used a plastic tube to transfer the water from the water samples to the glass bottle?**

Yes. Words added to text.

P4 L1: add reference for VINDTA-3C

The text states the make (Marianda) and model (VINDTA-3C) of the instrument that was used. There is no "reference" for the instrument.

L11: references for long-term changes: it seems like you have older refs than Steiner et al. 2018, please add

This is the only reference showing long-term changes in the Red Sea. Older references include older Red Sea data or some other aspect of Red Sea carbonate chemistry, but the aim of those studies was not to show long-term changes.

No changes made

L17: add the word "observed" so the sentence reads "describing the linear variations of observed S, TA and DIC ..."

Changed.

"describing the linear variations of S, TA and DIC ..." to "describing the linear variations of observed S, TA and DIC ..."

L19: define D here (distance from a defined zero point in the southern Red Sea)

Changed.

D is now defined earlier.

First paragraph of 2.4 now reads:

"A single-end-member mixing model was used to model conservative TA (cTA) and conservative DIC (cDIC) for coastal observations. First, the perpendicular distance of a point along the central axis of the Red Sea in km (D) was calculated for each observation. This was done using the "alongTrackDistance" function (default settings) in the R package "geosphere" (Hijmans, 2017) with the reference point 12.7737°N 43.2618°E to represent D = 0 and the reference point 28.2827°N 34.0694°E to define position of the central south-north axis. The single-end-member model was then implemented by 1) describing the linear variations of S, TA and DIC with D, so that predictions of offshore S (S_O), offshore TA (TA_O) and offshore DIC (DIC_O) can be made from D corresponding to coastal observations, and then 2) calculating cTA and cDIC for coastal observations according to Equations 1-2, which predict the simple dilution and concentration (SDC) effects of coastal evaporation (Figure 2)."

L19: explain difference between observed S, TA and DIC and predictions of So, Tao, and DICo (both along the north south axis). Why don't you use observed offshore values in Eq 1 and 2?

It is true we do use offshore observations in the methods to calculate 99% P.I. Thus the specification of only coastal observations being used in the model has been removed.

Section 2.4 (now 2.5) now reads:

2.5 Implementing a single-end-member mixing model

A single-end-member mixing model was used to model conservative TA (cTA) and conservative DIC (cDIC) for coastal observations. First, the perpendicular distance of a point along the central axis of *the Red Sea in km (D) was calculated for each observation. This was done using the "alongTrackDistance" function (default settings) in the R package "geosphere" (Hijmans, 2017) with the reference point 12.7737°N 43.2618°E to represent D = 0 and the reference point 28.2827°N 34.0694°E to define position of the central south-north axis. The single-end-member model was then implemented by 1) describing the linear variations of observed offshore S, TA and DIC with D, so that predictions of offshore S (S_O), offshore TA (TA_O) and offshore DIC (DIC_O) can be made from D corresponding to coastal observations, and then 2) calculating cTA and cDIC for observations according to Equations 1-2, which predict the simple dilution and concentration (SDC) effects of evaporation (Figure 2).*

Equation 1: $cTA = (S/S_O)*TA_O$

Equation 2: $cDIC = (S/S_O)* DIC_O$

Where S is the observed salinity at a coastal observation point and S_O, TA_O and DIC_O are calculated for a distance D corresponding to the observation point from the linear relationships found in step 1.

Other carbon parameters, the partial pressure of CO_2 (pCO_2), pH, the saturation state of aragonite (Ω_{Ar}), were calculated with the R package "seacarb" (Gattuso et al. 2018) assuming silicate and phosphate concentrations of zero, employing the total scale for pH and using the carbonate constants from Millero et al. (2010). Both conservative values and observed values were calculated for other carbon parameters, from cTA and cDIC, and observed TA and DIC, respectively.

Residual TA (rTA) and residual DIC (rDIC) were then calculated by subtracting cTA and cDIC from observed TA and observed DIC, respectively. Residual other carbon parameters ($rpCO_2$, rpH, $r\Omega_{Ar}$) were calculated by subtracting conservative values of other carbon parameters (calculated from cTA and cDIC) from observed values of other carbon parameters (calculated from TA and DIC observations).

L31: "All other open waters" means 200m< transition<coastal? And would you please define coastal?

A new section 2.4 has been added into the manuscript:

2.4 Definition of the coastal zone

Offshore observations used to describe the offshore end-member were those (from KAUST, WHOI and published sources) with bathymetry > 200 m below sea-level according to the General Bathymetry Chart of the Oceans (GEBCO) gridded bathymetry with a 30s resolution (BODC, https://www.bodc.ac.uk/). All other open-water observations not collected over a coastal habitat were labelled as coastal, transition waters. Samples collected over a coastal habitat were classified by the corresponding habitat, either coral reef, seagrass meadow or mangrove forest.

P5 L2: what is an "observed estimate"

Changed to "observed value"

Now reads:

Other carbon parameters, the partial pressure of CO_2 (pCO_2), pH, the saturation state of aragonite (Ω_{Ar}), were calculated with the R package "seacarb" (Gattuso et al. 2018) assuming silicate and phosphate concentrations of zero, employing the total scale for pH and using the carbonate constants from Millero et al. (2010). Both conservative values and observed values were calculated for other carbon parameters, from cTA and cDIC, and observed TA and DIC, respectively.

Residual TA (rTA) and residual DIC (rDIC) were then calculated by subtracting cTA and cDIC from observed TA and observed DIC, respectively. Residual other carbon parameters (rpCO_2, rpH, rΩ_{Ar}) were calculated by subtracting conservative values of other carbon parameters (calculated from cTA and cDIC) from observed values of other carbon parameters (calculated from TA and DIC observations).

L6: to ensure clarity, add "coastal" to "observed TA and observed DIC"

Not changed as coastal specification removed as above.

L18: change "two-end-member" with "single-end-member"

Thankyou

Changed "two-end-member" to "single-end-member"

L20: as above

Thank you

Changed "two-end-member" to "single-end-member"

L29: suggest changing "linear trends with D for S ...variables" with "how S, temperature and carbonate variables vary along the central axis from south to north".

The sentence has been adjusted to make it more explicit what linear relationships with D mean.

This sentence now reads:

Least squares regression analysis was used to calculate linear relationships with D for S, temperature and carbonate variables, thus determining how S, temperature and carbonate variables vary along the central axis from south to north

L30: add "to" between the words "used investigate"

Thank you!

"to" added between "used" and "investigate"

P7 L3: suggest a simpler language: "The offshore carbonate system of the Red Sea was characterized along the south-north ...".

Thank you!

P7 L3 now reads:

The offshore carbonate system of the Red Sea was characterized along the south-north central axis.

L4: suggest "Offshore waters exhibited significant and strong (highr2) linear increase in S ...". This sequence of words should be use all over , because the words "strong" or "weak" are connected to the linearity and only indirectly to significance.

Noted.

Changed "….strong (high r^2), significant…" *to "…. Significant and strong (high* r^2)….." *(and variations with "weak") everywhere.*

L6, L9, L10, L11: as above Are the strong/weak linear trend values summarized in a Table? If so , this should be announced early in paragraph 3.1.

Noted.

Table S3 reference added at the start of Section 3.1

L32: you describe the "Coastal observations", but then the word "central axis" should be exchanged with something else, since the coast is not along the central axis. Maybe just use "from south to north".

Noted.

Sentence now reads:

Coastal observations also displayed significant linear relationships with S from south-north along the Red Sea (Figure 3-5).

L37: change "end-member" with "waters"

Noted.

Changed "end-member" to "waters"

P8L7, L10, L14, L18, L19, L22andmore: as above. In general, I advise you to not use "end-member" when you mean "saters". It is just confusing.

Noted.

Changed "end-member" to "waters" in section 3.2 and where appropriate in the text. "offshore end-member" is now only used when referring to the single-end-member mixing model and not when comparing to offshore observations.

L31: do you really mean "trend", if so, over which time. If not, change with "linear relationship"

Addressed above

P9 L15: you are comparing to a "norm", are you referring to anomalies (P2, L12) or expected conservative behaviour (P2, L23)?

Comparing to the expected conservative behaviour using a 99% P.I. for error

Changed to 99% P.I.

L18: as above

As above

L22: delete "norm or"

Changed.

L24 and 25 ant the rest of this and next paragraphs: use other words for "norm"

Changed.

Here we are comparing to 99% P.I. so we have now changed the language to directly say this by replacing "norm" with "99% P.I.".

P10 L15: you write "seasonal trend", do you actual mean "seasonal variation"? If so, change all over

Addressed above.

Changed to "seasonal dependency"

P21 L5: change "The latitude at which time series stations are at is indicated by the text"Ts"" with "Time series stations are indicated as TS". Refer to Figure S1 in the figure text

Changed as suggested.

P22, Figure 2: define Oi earlier in figure text.

We have mentioned Oi earlier in the text

Now reads:

"……Flow axis 1 is along the south-north central axis where waters experience cumulative changes due to basin-scale evaporation and calcification. Flow axis 2 is perpendicular to this axis, where it is assumed that evaporative effects prevail as waters transition from offshore locations (Oi) to coastal regions."

L7: change "estimate" with "determine"

Changed as suggested.

L9: after "central axis at distance Di" add "from a fixed reference point in the southern Red Sea"

Changed as suggested.

P23, Figure 3: L3: suggest text " Offshore observations of S, T and carbon variables (left) and four coastal ..."

Changed as suggested.

P24, Figure 4: L3: change "end-members" with "waters"

Changed as suggested.

L4: after "included" add "in the"

Changed as suggested.

P26, Figure 6: A, B, C, D, AB, BC, CD are not explained

Noted.

Figure 7 caption changed from "Grouping letters indicate the results of post-hoc bootstrapped t-tests, summarized from statistics presented in Table S5. If tests showed significant similarities at the 0.05 significance level with another habitat across a variable they were assigned the same letter." to "Grouping letters (A-D) assigned above boxplots indicate the results of post-hoc bootstrapped t-tests, summarized from statistics presented in Table S5. If tests showed significant similarities at the 0.05 significance level with another habitat across a variable they were assigned the same letter."

Table S2: in the footnote you use a * as a multiplicator, this is confusing since the same sign is used as footnote numbering.

Noted

Changed footnotes +

Please change Table S3 and S4: please include units where you can (T, TA, DIC, pCO2 etc).

Noted.

Added unit references. Also added unit references to Table S2.

Table S4: change title from “By Habitat descriptive statistics for carbon variable habitat groups for all coastal ...” to “Descriptive statistics for carbon variable habitat groups for all coastal ...”

Noted.

Reviewer suggested change implemented.

Table S5: add units where feasible

Noted.

Added unit references

Table S7: as above

Noted.

Added unit references

Marked up Manuscript

Anomalies in the Carbonate System of Red Sea Coastal Habitats

Kimberlee Baldry[1*], Vincent Saderne[1], Daniel C. McCorkle[2], James H. Churchill[2], Susana Agusti[1] and Carlos M. Duarte[1]

[1] Red Sea Research Center and Computational Bioscience Research Center, King Abdullah University of Science and Technology (KAUST), Thuwal, 23955, Saudi Arabia
[2] Woods Hole Oceanographic Institution, Woods Hole, Massachusetts 02543, USA
[*] Current affiliation: Institute of Marine and Antarctic Studies, University of Tasmania, Hobart 7000, Australia

Correspondence to: Kimberlee Baldry (kimberlee.baldry@utas.edu.au)

Abstract. We use observations of dissolved inorganic carbon (DIC) and total alkalinity (TA) to assess the impact of ecosystem metabolic processes on coastal waters of the eastern Red Sea. A simple, single-end-member mixing model is used to account for the influence of mixing with offshore waters and evaporation/precipitation, and to model ecosystem-driven perturbations on the carbonate system chemistry of coral reefs, seagrass meadows and mangrove forests. We find that 1) along-shelf changes in TA and DIC exhibit strong linear ~~trends~~ relationships that are consistent with basin-scale net calcium carbonate precipitation; 2) ecosystem-driven changes in TA and DIC are larger than offshore variations in >7~~8~~0~~5~~% of sampled seagrass meadows and mangrove forests, changes which are influenced by a combination of longer water residence times and community metabolic rates; and 3) the sampled mangrove forests show strong and consistent contributions from both organic respiration and other sedimentary processes (carbonate dissolution and secondary redox processes), while seagrass meadows display more variability in the relative contributions of photosynthesis and other sedimentary processes (carbonate precipitation and oxidative processes).

1. Introduction

Coral reefs, seagrass meadows and mangrove forests are sites of intense metabolic processes. These habitats are distributed heterogeneously in the coastal zone, at shallow depths where perturbations in the carbonate system by metabolic processes can have the greatest influence on water chemistry and air-sea carbon dioxide (CO_2) exchange (Bauer et al., 2013~~;~~; Camp et al., 2016~~;~~; Cyronak et al., 2018~~;~~; Gattuso et al., 1998~~;~~; Guannel et al., 2016~~;~~; Unsworth et al., 2012).

The cumulative impact of coastal habitats on the carbonate system, along with their overall importance in the global carbon cycle, is difficult to quantify and is poorly represented when compared to knowledge of open ocean processes (IPCC, 2014). The open ocean is geographically separated from the benthos and land so their respective influences on the carbonate system often can be ignored over short time-scales. In addition to the influence of metabolism in coastal habitats, the carbonate system of the coastal zone is also influenced by both the benthos and ~~the~~ land over short time-scales. Thus, terrestrial and freshwater inputs (dissolved and particulate), sediment exchanges, biological processes, and changes in circulation and water residence time must all be considered when studying perturbations in the carbonate system of the coastal zone (Doney, 2010~~;~~; Duarte et al., 2013~~;~~; Giraud et al., 2008~~;~~; Jiang et al., 2014~~;~~; IPCC, 2014).

Changes in carbonate system concentrations in the coastal zone can be conservative or non-conservative (Jiang et al., 2014). Conservative changes arise from the mixing of water masses and from evaporation. The salinity of a water mass is a conservative property and can be used to estimate the conservative component of changes in carbonate system concentrations. The conservative mixing of coastal water masses is often conceptualized as a two-end-member problem; with changes in carbonate system concentrations linearly related to salinity between a freshwater end-member (e.g. rivers, land run-off) and an offshore oceanic end-member (Jiang et al., 2014~~;~~; Robbins, 2001). Non-conservative changes in the coastal zone are driven by metabolic processes, sediment exchanges and land inputs (Duarte et al., 2013~~;~~; Jiang et al., 2014). As such, these non-conservative changes can be measured as ~~departures, or~~ anomalies ~~, from a “norm” defined by the expected carbonate system resulting from~~in the carbonate system ~~which has experienced~~relative to conservative mixing.

The lack of significant freshwater inputs, via rivers and rainfall, in the arid Red Sea means that offshore waters are the only source of mixing exchange to the coastal zone, allowing for the implementation of a ~~single~~ single-end-member mixing model (Sofianos and Johns, 2003). A constant oceanic salinity for the offshore region cannot be used to model conservative behaviour, due to basin-scale evaporation which causes a south~~-to~~-north increase in salinity along the central axis of the Red Sea. The observed south~~-to~~-north increase in alkalinity is smaller than ~~would be predicted for~~ conservative behaviour predicts, ~~as a result of~~ due to chemeogenic and biogenic calcium carbonate ($CaCO_3$) precipitation throughout the Red Sea (Jiang et al., 2014~~;~~; Steiner et al., 2014~~;~~; Steiner et al., 2018~~;~~; Wurgaft et al., 2016). Thus, the linear ~~trend~~ relationships in offshore carbonate system concentrations, combined with the additional variability of coastal evaporation, defines ~~the “norm” or~~ the expected conservative behaviour for the entire coastal zone of the Red Sea (Figure 1).

Here we explore the carbonate system in the eastern (Saudi-EEZ) coastal zone of the Red Sea. We examine concentrations of total alkalinity (TA) and dissolved inorganic carbon (DIC) over and around coral reefs, seagrass meadows and mangrove forests, and compare these to the same properties measured in offshore Red Sea surface waters. By using a simple single-end-~~–~~member mixing model, that accounts for conservative changes in the carbonate system of the coastal zone, we detect large ecosystem-driven anomalies in coastal habitats. Smaller non-conservative changes, particularly characteristic of coral reefs, were not able to be detected with high confidence using the over-simplified circulation model but could be resolved with more knowledge of offshore circulation and variability of the carbonate system in the Red Sea.

2. Methods

2.1 KAUST Observations

Between February 2016 and August 2017, seawater samples were collected in the Red Sea during daylight hours from six oceanographic cruises (January/February 2016, January/February 2017, March 2017, April 2017, May 2017, July/August 2017) and at coastal time series stations (Figure 1, Table S1). The six oceanographic cruises visited ~~the~~ three types of shallow coastal habitats, spanning the full length of the Saudi-EEZ coast. Open-water samples were also collected on cruises at a distance from (ie. not directly above, or beside) ~~the three~~ shallow coastal habitats. The coastal time series sampling of surface waters was conducted every two weeks at four stations near the King Abdullah University of Science and Technology (KAUST): a transition water station (22.3093°N 38.9974°E, n = 31), a coral reef station (22.25285°N 38.96122°E, n = 32), a mangrove forest station (22.3394°N 39.0885 °E, n = 23) and a seagrass meadow station (22.3898°N 39.1355 °E, n = 32) (Figure S1).

Transition and offshore water samples were collected using a Niskin bottle deployed off the side of the vessel, together with temperature (T) and salinity (S) recorded with an Ocean Seven 305Plus multi-parameter conductivity-temperature-depth (CTD) instrument. Seawater samples ~~collected over~~from coastal habitats were collected in close proximity to the habitat with a 10 cm diameter by 30 cm long polyvinyl-chloride cylinder, to avoid disturbing the benthic organisms and the associated re-suspension of sediments or epiphytes. The cylinder was carefully moved over the ecosystem and sealed with rubber caps. Measurements of S and T were made at the sampling point using a hand-lowered Ocean Seven 305Plus multi-parameter CTD instrument. The cylinders were then transported to the vessel where water was carefully siphoned using a silicone tube.

Water samples were collected into 12 ml glass vials (DIC) and 50 ml plastic falcon tubes (TA), for all cruises except one (Cruise ID = CSM16) during which TA samples were collected in 12ml glass vials. To halt biological activity, DIC and TA samples were poisoned to a concentration 0.02 % mercuric~~y~~ chloride solution. TA and DIC were measured at KAUST according to the standard operating procedures as set out by Dickson et al. (2007). DIC was measured by an infrared technique with an Appolo SciTech AS-C3 DIC analyser, and TA was measured by open-cell titration with 0.1 M hydrochloric acid using a Mettler Toledo T50 Autotitrator equipped with an InMotion Pro Autosampler using non-linear curve fitting to determine an equivalence point. Both measurements were standardized using certified reference materials (CRM) obtained from Dr. A~~A.~~ndrew Dickson (Scripps Institute of Oceanography). Observations were flagged based on the standard error between replicates, and those that had only single replicates or high standard error (SE > 20 µmol ~~/~~kg^{-1}) were excluded from further analysis (n = 17).

2.2 WHOI Observations

Two oceanographic cruises led by the Woods Hole Oceanographic Institution (WHOI) were conducted in March 2010 and September/October 2011. Targeting open waters of the Red Sea, the cruises traversed the length of the Saudi-EEZ coast. T and S observations were acquired using the ship's CTD, and water samples were collected using Niskin bottles on the CTD rosette. On deck, water samples were transferred into 250 -ml glass bottles using a length of silicone tubing, taking care to minimize exchange with the atmosphere, and were poisoned with 50 µL of a saturated mercuric chloride solution immediately after acquisition. The samples were analysed at WHOI for TA and DIC using a Marianda VINDTA-3C analysis system. TA was determined by non-linear curve fitting of data obtained by open-cell titrations, and DIC concentrations were determined by coulometric analysis, according to the standard operating procedures as set out by Dickson et al. (2007). Both measurements were standardized using CRM obtained from Dr. A. Dickson. The difference between replicate samples averaged 0.6 and 1.5 µmol kg^{-1} for alkalinity and 3.0 and 2.7 µmol kg^{-1} for DIC, for the 2010 and 2011 cruises, respectively.

2.3 Published Data-Sets

Open-water surface observations (<50m) collected over 2007-2010 were sourced from published data-sets (Table S1). Data was constrained to a comparable area of the Red Sea in which new observations collected by KAUST and WHOI were obtained (17-28 °N, 30-44°E). ~~We elected to only use data collected within a decade of coastal observations (2007-2010), as long-term changes were observed in carbonate variables in the Red Sea. This observation has been recently confirmed by~~A recent study by Steiner et al. (2018) detected differences between new Red Sea TA observations obtained in 2015/6 and 2018, and old Red Sea TA observations from a 1998 cruise on the RV Sea Surveyor (Steiner et al. 2014). We reassess these differences between old and new Red Sea data using the data from Steiner et al. (2018), the RV Sea Surveyor, WHOI data (this study) and data collected from 1982 aboard the RV Marion Durfresne (Papaud and Poisson, 1986). ~~We~~ Consequently, we elected to only use data collected within a decade of coastal observations (2007-201~~0~~7) for our study, as long-term changes were observed in carbonate variables in the Red Sea (Figure 3).

2.4 Definition of the coastal zone

~~Offshore observations used to describe~~The stations used to define the offshore end-member were those (from KAUST, WHOI and published sources) with b~~athymetry~~ottom depths > 200 m ~~below sea level~~ according to the General Bathymetry Chart of the Oceans (GEBCO) gridded bathymetry with a 30 s resolution (BODC, https://www.bodc.ac.uk/). All other open-water observations (i.e., stations with bottom depths < 200 m and not collected over a coastal habitat) were labelled as coastal, transition waters. Samples collected over a coastal habitat were classified by th~~at~~e corresponding habitat ~~type~~, either coral reef, seagrass meadow or mangrove forest.

2.54 Implementing a single-end-member mixing model

A single-end-member mixing model was used to model conservative TA (cTA) and conservative DIC (cDIC) for coastal observations. First, t~~T~~he ~~perpendicular~~ distance of a point along the central axis of the Red Sea in km (D) was calculated for each observation. This was done using the "alongTrackDistance" function (default settings) in the R package "geosphere" (Hijmans, 2017) with the reference point 12.7737°N 43.2618°E to represent D = 0 and the reference point 28.2827°N 34.0694°E to define position of the central south-north axis. ~~This was achieved by~~The single-end-member model was then implemented by -1) describing the linear variations of offshore S, TA and DIC with ~~along the south-north central axis of the Red Sea (~~D~~)~~, so that predictions of offshore S (S_O), offshore TA (TA_O) and offshore DIC (DIC_O) can be made from the value of D corresponding to coastal observations, and then 2) calculating cTA and cDIC for ~~coastal~~ observations according to Equations 1-2, which predict the simple dilution and concentration (SDC) effects of ~~coastal~~ evaporation (Figure 2).

Equation 1: $cTA = (S/S_O)*TA_O$

Equation 2: $cDIC = (S/S_O)* DIC_O$

Where S is the observed salinity at a coastal observation point and S_O, TA_O and DIC_O are calculated from the linear relationships found in step 1, for a distance D corresponding to the ~~coastal~~ observation point. ~~from linear trends found in step 1.~~

~~Offshore observations used to describe the offshore end-member were those (from KAUST, WHOI and published sources) with bathymetry > 200 m below sea level according to the General Bathymetry Chart of the Oceans (GEBCO) gridded bathymetry with a 30s resolution (BODC, https://www.bodc.ac.uk/). All other open-water observations were labelled as transition waters. The distance along the central axis of the Red Sea in km (D) was calculated for each observation using the "alongTrackDistance" function (default settings) in the R package "geosphere" (Hijmans, 2017) with the reference point 12.7737°N 43.2618°E to represent D = 0 and the reference point 28.2827°N 34.0694°E to define position of the central south-north axis.~~

Other carbon parameters ~~(OCP's),~~ , the partial pressure of CO_2 (pCO_2), pH, the saturation state of aragonite (Ω_{Ar}), were calculated with the R package "seacarb" (Gattuso et al. 2018) assuming silicate and phosphate concentrations of zero, employing the total scale for pH and using the carbonate constants from Millero et al. (2010). Both conservative mixing ~~estimates~~ values and observed ~~estimates~~ values were calculated for ~~OCP's~~other carbon parameters ~~at coastal locations~~, from cTA and cDIC, and observed TA and DIC, respectively.

Residual TA (rTA) and residual DIC (rDIC) were then calculated by subtracting cTA and cDIC from observed TA and observed DIC, respectively. Residual ~~OCP's~~other carbon parameters (rpCO_2, rpH, r-Ω_{Ar}) were calculated by subtracting conservative value~~estimate~~s of ~~OCP's~~other carbon parameters (calculated from cTA and cDIC) from observed ~~estimates~~ values of ~~OCP's~~other carbon parameters (calculated from TA and DIC observations).

2.6~~5~~ Model Assumptions and Limitations

The single-end-member mixing model assumes simple two-dimensional circulation in a region that exhibits more complex flow. The modelled flow follows a south-~~to n~~north trajectory along the central axis of the Red Sea, with perpendicular coastal flushing from offshore waters located at similar distances along the central axis (Figure 2). This allows changes in the carbonate chemistry of offshore waters, due to both conservative and non-conservative processes, and conservative coastal evaporation to be modelled.

~~It is well known that this is not the case~~This is a substantial simplification – in fact, ~~and~~ the Red Sea has a complex surface flow displaying multiple dynamic eddies along its length (Sofianos and Johns, 2003~~;~~, Zhan et al., 2014).

Depending on the direction of flow, these eddies promote coastal flushing from offshore waters originating further north or further south along the central axis of the Red Sea, mixing in a way the simple ~~two~~single-end-member mixing model cannot capture.

Other limitations of the simple ~~two~~single-end-member mixing model include its inability to account for coastal upwelling along the continental shelf, variable mixing of Gulf of Aden waters with Red Sea offshore waters and changes in ~~basin scale~~basin-scale evaporation and calcification which have been documented in previous studies (Anderson and Dyrssen, 1994~~;~~; Churchill et al., 2014~~;~~; Krumgalz et al., 1990~~;~~; Papaud and Poisson, 1986~~;~~; Steiner et al., 2018).

These limitations cannot be addressed within the present study and would require a sustained observational effort to address knowledge gaps in the carbon chemistry of the Red Sea, combined with more complex circulation models. Complex circulation models could capture some large-scale variance in circulation, but they are costly simulations, that may still produce questionable results due to the unresolved coastal bathymetry of the Red Sea. Instead, we use the 99% prediction interval (P.I.) of offshore carbonate chemistry residuals as a bound of model error, and to capture deviations from modelled carbonate chemistry due to the predescribed variations in mixing. ~~These limitations cannot be addressed within the present study and require a sustained observational effort to address knowledge gaps in the carbon chemistry of the Red Sea, combined with more complex circulation models.~~

2.7~~6~~ Statistical tests

All statistical tests were performed using R software (R core team, 2017) with a 95% confidence level. Least squares regression analysis was used on a spatial data subset (all observations excluding time-series) to calculate linear ~~trends~~ relationships with D for S, temperature and carbonate variables, thus determining how S, temperature and carbonate variables vary along the central axis from south~~-to-~~–north. Least squares regression analysis was also used to calculate relationships between rTA and rDIC. The square of Pearson’s correlation coefficient (r^2) was used to evaluate the strength of the linear relationships. Least squares analysis of variance (LS-ANOVA) was ~~also~~ used to investigate interaction effects between D and habitat groups to test for significant differences between linear regression slopes with D across habitats for S~~S~~, temperature and carbon variables.

Seagrass meadows and mangrove forests displayed greater variances compared to other groups (maximum variance/minimum variance > 2) between carbon variables, violating the assumption of homoscedasticity between groups required for parametric analysis of variance. For this reason, a Wilcox’s robust ANOVA (WR-ANOVA) was chosen to account for heteroscedasticity across habitat groups. WR-ANOVA’~~'~~s for differences in medians were conducted between observations from offshore waters, transition waters and coastal habitats. Tests between medians were chosen, rather than between means, as mangrove habitats displayed skewed TA and DIC observations. Wilcox’s robust statistical methods were implemented using the R package “WRS2” (Mair and Wilcox 2018), with the functions “med1way” for testing differences in medians and a bootstrapped t-test employed (Supplementary R Code) for post-hoc analysis.

To assess the strength of seasonal cycles at time series stations and to test differences ~~in~~ between habitats, a seasonal proxy (SP) was constructed from temperature observations at the transition and coral reef time series stations. A cubic smoothing spline, with a smoothing parameter of 0.55, was fit to three iterations of the temperature seasonal cycle at the ~~coral reef~~ stations. The fit was then scaled such that a value of 1 indicates peak summer period, and a value of -1 indicates peak winter period. Parametric tests were chosen to detect correlations with season, as variances across season were roughly homoscedastic. LS-ANOVA was used to assess the significance of seasonal cycle as a predictor in time-series observations, to infer the presence of interaction effects between habitats and season in time-series observations, and to infer differences in rTA:rDIC slopes between time series observations and spatial observations. WR-ANOVA was also performed on time series observations to assess median differences between the four time series stations.

3. Results

3.1 The Red Sea offshore end-member

The offshore carbonate system of the Red Sea ~~offshore end-member~~ was characterized along the south-north central axis. Offshore waters exhibited significant and strong (high r^2)~~, significant~~ linear increases in S, TA and DIC along the central south-north axis of the Red Sea as indicated by respective regression analysis with D (Figure ~~3~~4, Table S3). TA and DIC were normalized to a salinity of 35 (nTA and nDIC), and both exhibited significant and weak~~, significant~~ (low r^2) linear decreases along the central south-north axis of the Red Sea (Figure ~~4~~5). However, winter nDIC values appear to deviate from this ~~trend~~linear relationship. The nTA and nDIC co-varied along this axis in an average ratio of 0.69~~63~~ (SE= 0.06~~6~~, r^2 = 0.60~~52~~, F = ~~95.8~~147.7, p<0.001) nTA to 1 nDIC (Figure 5~~4~~c). A significant and weak (low r^2)~~, significant~~ linear decrease was found for T against D, that displayed clear seasonal dependencies between summer and winter/spring temperatures (Figure 4). A significant and weak (low r^2)~~, significant~~ increase in pH, a significant and weak (low r^2)~~, significant~~ decrease in pCO_2, and no significant ~~trend~~ linear relationship in Ω_A, against D were also observed.

In defining the offshore end-member for implementation in the single-end-member mixing model, offshore observations not representative of the expected ~~trends~~ linear relationships in the surface offshore Red Sea were removed (n = 11). These were identified as ~~nine~~ eleven outlying offshore observations exhibiting a Cook's distance greater than five times the mean in at least one of the three linear models of D, against S, TA and DIC (Figure 1; ~~(~~Cook and Weisberg, 1997~~)~~). Linear models were then re-fit with the remaining offshore observations (n = 104~~92~~) to yield Equations 3-5, to be substituted into Equations 1-2 to complete the single-end-member mixing model (Figure ~~3~~2).

Equation 3: S_O = 0.~~00147~~00157*D + 37.~~62~~47

Equation 4: TA_O = 0.~~04970~~0510*D + ~~2408~~2407

Equation 5: DIC_O = 0.0437*D + ~~2027~~2029

To approximate the error of the single-end-member mixing model, 99% prediction intervals (99% P.I. = mean ± 2.576*sd) were calculated by applying the single-end-member mixing model to offshore observations to yield rTA, rDIC, rpCO_2, rpH and rΩ_{Ar} (Table S2). These 99% P.I. represent a cumulative error due to the natural variations of S_O, TA_O and DIC_O, along with the error propagation associated with the calculations of ~~OCP~~other carbon parameters. Two offshore observations used in defining the offshore end-member ~~the norm~~ fell outside the 99% P.I., both exhibiting high TA, and one exhibiting high DIC.

3.2 The Red Sea Coastal Zone

Coastal observations also displayed significant ~~spatial trends~~linear relationships ~~in~~ with S ~~along the~~from south-north ~~central axis of the~~ Red Sea (Figure ~~3-5~~4). At the transition and coral reef sites, increases in S with D were significant and of comparable strength (indicated by r^2 values) to those observed offshore, while a weaker (lower

r^2) increase in S with D was observed at seagrass meadows (Table S3). No significant increase in S with D was observed at mangrove forests. No interaction effects between habitat type and D were observed for S, meaning that rates of increases in S with D did not differ significantly between habitats or ~~the offshore end-member~~offshore waters (excluding mangrove forests; F = ~~0.94~~1.55, p = 0.~~395~~203). Consequently, it can be concluded that compared to offshore waters, irrespective to D, significantly higher median S were observed at mangrove forests across the Red Sea coastal zone ~~and seagrass meadows~~ (Figure 6). Similarly, it can be concluded that irrespective to D median S for ~~coral reef and~~ transition waters, coral reefs and seagrass meadows were comparable to the median S observed offshore.

Within coral reefs, seagrass meadows and mangrove forests, decreases in T with D were significant and stronger (higher r^2), compared to the decreases observed in offshore waters (Figure 4~~3~~, Table ~~S3~~S4). Tests for interaction effects indicated that rates of change of T with D differed significantly among habitats (F= ~~6.25~~7.54, p < 0.001), but these differences were small and did not deviate largely away from those observed in ~~the~~ offshore ~~end-member~~waters (Figure ~~3~~4). Transition waters displayed similar T to offshore waters along the entire length of the Red Sea. Differently, the three coastal habitats displayed on average slightly higher average T in the southern Red Sea, compared to ~~the~~ offshore ~~end-member~~waters (Figure ~~3~~4). There was a high sampling bias towards winter/spring in coastal observations and corresponding measurements of in-situ T were not successfully made for all summer observations, so the seasonal ~~trends~~ dependencies cannot be confidently compared or described here.

Compared to ~~the offshore end-member~~offshore waters, TA ~~and DIC~~ across transition, coral reef and seagrass meadow sites displayed similar rates of increases with D but differing median values and distribution (Figure ~~3~~4, Figure 6a). Increases in TA with D for each coastal habitat were ~~much~~ weaker (lower r^2) compared to those observed in offshore waters, with significant linear relationships present for all habitats but mangrove forests. There were no interaction effects between D and habitat groups (excluding mangrove forests ~~(~~; F = 0.~~10~~95, p = 0.~~903~~417), meaning that coastal TA displayed increased variability and similar rates of increase with D compared to ~~the~~ offshore ~~end-member~~waters. Although rates of increase of TA with D were similar between habitats and offshore waters, median TA was not. Compared to offshore waters, lower median TA was observed at seagrass meadows across the Red Sea coastal zone (Figure 4, Figure 6a).

Increases in DIC with D were also weaker (lower r^2) for coastal observations compared to ~~the~~ offshore ~~end-member~~waters, with significant linear relationships observed only for transition and coral reef waters. An ~~and exhibited no~~ interaction effect~~s~~ with D across habitat was observed (excluding mangrove forest and seagrass meadow; ~~habitats (~~F = ~~1.99~~4.66, p = 0.~~162~~011). Differences in how DIC changed with D, indicated by the presence of this interaction effect, was driven by coral reef DIC, which showed increased variability and was often lower when compared to offshore waters. There was a higher occurrence of low DIC in the Southern Red Sea, creating a difference in how DIC changed linearly with D compared to offshore and transition waters (Figure 4). Compared to offshore waters, transition waters and coral reefs showed small increased in median DIC, whilst~~. This means that coastal DIC displayed increased variability and similar rates of increase with D compared to the offshore end-member~~waters~~.~~

~~Although rates of increase of TA and DIC with D were similar between habitats and the offshore end-member~~waters~~, median TA and DIC were not. Compared to the offshore end-member~~waters~~, lower median TA was observed at transition, seagrass meadow and coral reef sites across the Red Sea (Figure 3, Figure 6a). Compared to the offshore end-member~~waters~~, lower median DIC was observed at seagrass meadows and coral reefs across the whole Red Sea, whilst transition waters displayed similar median DIC. Compared to the offshore end-member~~waters~~, observations of DIC at~~ mangrove forests displayed ~~similar~~ higher median DIC ~~but displayed~~with ~~much~~ higher variability around this median (Figure 6a).

Observations of pH and pCO_2 showed statistically significant, but relatively weak (low r^2), ~~trends~~ linear relationships with D for only seagrass meadow and coral reef sites (Figure 4~~3~~, Figure 6a). No interaction effects were observed between these habitats and offshore waters meaning that rates of change with D were statistically similar (excluding transition water and mangrove forest; F = 1.54~~0.18~~, ~~0.45~~1.98, p = 0.~~670~~217, 0.~~503~~141 for pH and pCO_2 respectively). Compared with ~~the~~ offshore ~~end-member~~waters, pH and pCO_2 at coral reefs showed statistically similar medians and greater variability. Compared to ~~the~~ offshore ~~end-member~~waters, mangrove forest and seagrass habitats displayed lower median pH and higher median pCO_2, and greater variability. Compared to ~~the~~ offshore ~~end-member~~waters, transition observations displayed slightly lower median pH and higher median pCO_2, and greater variability. As seen in ~~the~~ offshore ~~end-member~~waters no significant ~~trends~~ linear relationships with D were observed for Ω_{Ar} at coastal habitats or transition waters, however coastal observations of Ω_{Ar} displayed lower medians and higher variability, compared to ~~the~~ offshore ~~end-member~~waters. Mangrove forests displayed the most variability in observed values across all carbon variables.

One outlying mangrove forest observation taken near KAUST in 2016 showed high TA values, and low DIC, leading to unrealistic estimations of other carbon parameters (Figure S2). Further, an isolated mangrove stand was sampled from an inland late that was tidally flushed (Figure S3a). The two observations taken from this mangrove stand contained much higher TA and DIC compared to observations from coastally residing mangrove stands. The outlying observation was excluded from analysis, however the observations from the inland mangrove stands were not.

~~One outlying mangrove forest observation showed high TA values, and low DIC, leading to unrealistic estimations of OCP's~~other carbon parameters ~~(Figure 5). This outlying observation was taken near KAUST in April 2016 and was most likely caused by sample handling error (degassing or the inclusion of sediments in sample). Further, an isolated mangrove stand was sampled from an inland late that was tidally flushed (Figure S2a). The two observations taken from this mangrove stand contained much higher TA and DIC compared to observations from coastally residing mangrove stands.~~

3.3 Coastal Ecosystem Anomalies

Using a simple single-end-member mixing model, large non-conservative carbonate system residuals were detected in the coastal Red Sea (Figure 6b). Slopes from least-squares linear regressions with D indicate that non-conservative carbonate system residuals display no significant ~~trends~~ linear relationships along the south-north central axis of the Red Sea (Table S3, Figure ~~S4~~S5). Compared to the ~~norm~~99% P.I., coral reefs ~~and mangrove forests~~ exhibited ~~similar~~lower median rDIC and lower median rTA, whilst transition waters exhibited similar median rTA and higher median rDIC, although differences were smallest at these sites. Changes at ~~and s~~seagrass meadows and mangrove forests were more pronounced, with a relatively larger variability. Compared to the 99% P.I., both habitats displayed lower median rTA, however lower median rDIC was observed at seagrass meadows whilst higher median rDIC was observed at mangrove forests. ~~exhibited lower median rTA and lower median rDIC (Figure 6b). Variability in rTA and rDIC was much larger than the 99% P.I. for seagrass meadows and mangrove forests, but not for, compared to the variability of the norm, coral reefs and transition waters.~~

Non-conservative carbonate system residuals that fall outside of 99% P.I. deviate significantly away from the ~~norm or~~ expected conservative behaviour of the coastal zone and are concluded to be ecosystem-driven anomalies in the carbonate system (Figure 6b). Transition waters displayed the lowest occurrences of ecosystem-driven anomalies, that were equally distributed towards higher rTA and lower rTA compared to the ~~norm~~99% P.I., and mostly towards higher rDIC compared to the ~~norm~~99% P.I.. Coral reefs also displayed a relatively low range of rTA and rDIC ecosystem-driven anomalies, equally distributed to higher and lower values ~~when compared to the norm99% P.I.s~~ for r~~both~~ TA compared to the 99% P.I., and mostly towards lower rDIC compared to the 99% P.I.. ~~There was a similar occurrence of DIC ecosystem-driven anomalies in coral reefs that were equally distributed towards higher DIC and lower DIC compared to the norm99% P.I.~~ Seagrass meadows and mangrove forests displayed markedly higher occurrences of ecosystem-driven anomalies compared to transition waters and coral reefs. Seagrass meadows displayed ecosystem-driven anomalies distributed mostly towards lower rTA compared to the ~~norm~~99% P.I., and rDIC ecosystem-driven anomalies distributed mostly towards lower rDIC values compared to the ~~norm~~99% P.I.. Mangrove forests displayed ecosystem-driven anomalies distributed mostly towards lower rTA compared to the ~~norm~~99% P.I., and ~~DIC~~ ecosystem-driven anomalies distributed ~~equally above and below~~mostly towards higher rDIC compared to the ~~norm~~99% P.I..

Coastal observations of ~~OCP's~~other carbon parameters displayed lower median rpH, higher median rpCO_2 and lower rΩ_{Ar} compared to the ~~norm~~99% P.I.. Differences in ~~OCP~~other carbon parameters compared to the ~~norm~~99% P.I. were most pronounced and displayed a large variability in mangrove forests. A significant proportion of ecosystem-driven anomalies in ~~OCP's~~other carbon parameters was detected at all coastal habitat types. In transition waters, mangrove forests and seagrass meadows, these ecosystem-driven anomalies were mostly observed to have lower pH, higher pCO_2 and lower Ω_{Ar} compared to the ~~norm~~99% P.I.. Compared to the ~~norm~~99% P.I., coral reef observations exhibited a relatively equal distribution of both high and low ecosystem-driven anomalies in pH, a small number of high ecosystem-driven anomalies in pCO_2 and low ecosystem-driven anomalies in Ω_{Ar}.

3.4 Coastal Time Series

Despite their proximity, there were significant differences in temperatures and S between the three coastal time series sites (Figure 7, Table S6). The coral reef and transition stations displayed similar S of comparable variability, exhibiting no variation with season. Observations of S at the seagrass meadow station were higher, and more variable than those observed at coral reef and transition stations. A seasonal ~~trend dependancy~~dependency in S was indicated by correlation with the seasonal proxy at this station, however, the correlation is weak and the cycle exhibits a small amplitude. The mangrove forest displayed the highest S, exhibiting no relationship with season and higher variability compared to the coral reef and transition stations.

Strong seasonal ~~trends~~ dependaencies in T were observed at all four time series stations. The seasonal cycles exhibited slower rates of decreases in T towards winter and larger rates of increase in T towards summer. The interaction effect between habitat and the seasonal proxy was significant, indicating that seasonal cycles of T changed between habitat ($F = 3.99$, $p = 0.01$). Compared to the transition and coral reef stations, the T observed at the seagrass stations was often higher in winter, and lower in summer, whilst T observed at the mangrove forest station was only higher in summer (Figure 7, Figure S4~~3~~).

The coral reef and transition stations displayed a similar series of observations of TA, DIC and their respective residuals. The seagrass meadow station was the only station at which strong, statistically significant seasonal cycles, were observed in both TA and DIC. During summer, the TA and DIC were lower at the seagrass meadow station compared transition and coral reef stations; whereas similar TA and DIC were seen at all stations during winter. Similarly, during summer rDIC was lower at the seagrass meadow station compared to that observed at the transitions and coral reef stations, but in winter rTA and rDIC did not completely return to values observed at the transitions and coral reef stations. Weak (low r^2), statistically significant seasonal cycles were observed at the seagrass station in pH and pCO_2, and at the transition station in DIC, although no clear deviations from other stations exist in these carbon variables. Compared to the other three stations, the mangrove forest station displayed no correlations with the seasonal proxy for all carbon variables, and exhibited much larger variability. TA and DIC at the mangrove forest station were similar to TA and DIC at transition and coral reef stations, indicated by differences in medians. However, rTA and rDIC at the mangrove forest station more closely resembled rTA and rDIC observed at the seagrass station than at the other two stations, as indicated by differences in medians. No large differences in medians were observed across ~~OCP's~~other carbon parameters and their respective residuals.

3.5 Relationship between rTA and rDIC

Slopes, intercepts and appropriate statistics are presented in Table 1 for linear regression analysis of transition waters, coral reefs, seagrass meadows and mangrove forests. The slope of the relationship between rTA and rDIC was similar between the time series observations and the spatial observations in transition waters, coral reefs and mangrove forests (F = 1.~~10~~.05, 1.~~13~~ 11 and 0.07 respectively, p = 0.~~297~~309, 0.~~291~~ 295 and 0.~~790~~ 794 respectively) but different in seagrass meadows (F = 6.~~41~~44, p = 0.014), as indicated by the significance of interaction effects between rDIC across observation subset for each habitat.

Transition water and coral reef observations displayed a significant and weak (low r^2) linear relationship between rTA and rDIC with an intercept close to zero. Seagrass meadow observations collected from the time-series station displayed significant and strong (high r^2) linear relationship~~s~~ between rTA and rDIC, but the spatial subset of observations did not. ~~over both subsets of data, with significant~~ There was a significant difference~~s~~ in slope of 0.36 and 0.73 ~~for~~ between the spatial and time series ~~observations~~ subsets respectively, with both regressions displaying similar negative rTA intercepts. The two observations from the inland mangrove stand deviated largely from the extrapolated linear relationships calculated using coastal mangrove stands, and as such were excluded from following regression analysis'. Mangrove forest observations displayed a significant and strong (high r^2) ~~strong, positive~~linear relationship between rTA and rDIC over both subsets of data, with a negative rTA intercept and a slope of 0.62 and 0.60 for spatial and time series observations respectively.

4. Discussion

The relatively simple oceanography of the offshore Red Sea, with only one oceanic end-member influencing a narrow basin, yields simple linear ~~trends~~ relationships in salinity (S), temperature (T), total alkalinity (TA), dissolved inorganic carbon (DIC), pH and pCO_2 along the south-north central axis (Figure ~~3~~4). The observed increases in TA along the central axis of the Red Sea were smaller than would be conservatively predicted from the central axis salinity data, consistent with previous studies which found that basin-scale calcification produces non-conservative deficits of TA that accumulate along the south-north central axis (Figure 5~~3~~; ~~(~~Jiang et al., 2014~~;~~; Steiner et al., 2014~~;~~; Steiner et al., 2018~~;~~; Wurgaft et al., 2016). The observed increases in DIC were also consistent with basin-scale calcification in summer/spring, but winter results showed more varience around this~~ trend~~ relationship. ~~These~~ These linear relationships in offshore ~~trends~~ waters are reflected in the water chemistry of the coastal zone and are removed with the use of a single-end-member conservative mixing model (Figure 2; Figure ~~S4~~S5). Doing so enables us to study non-conservative perturbations of carbonate system in shallow benthic habitats at a basin-scale.

To distinguish ecosystem-driven deviations in the carbonate system from conservative variability, conservative TA and DIC in the off-shore end-member is estimated and 99% P.I. are constructed for rTA and rDIC, from offshore observations (Table S2). This error bound captures offshore variability in in S, TA and DIC due to the effects of inter-annual differences, eddies and variable circulation patterns, which act along similar spatial scales in both the offshore and coastal zones. We expected to observe only evaporation-driven increases of S in the coastal zone, as freshening by land inputs and precipitation is thought to be not significant. Yet, roughly 25% of observations of S in coral reefs and transition waters were lower than those observed in ~~the~~ offshore ~~end-member~~waters, highlighting the simplifications inherent in the ~~one-~~single-end-member model (Figure ~~3~~4, Figure 6a). In winter, this observed freshening could be due to winter precipitation which is accounted for in the model. Alternatively, it could be due to effects that are not captured in the model, including seasonal rivers (wadis) caused by flash floods that occur mainly during October-May (de Vries et al., 2013~~;~~; Robbins, 2001). These flooding events have not been explored in the context of TA and DIC inputs. In summer, the observed freshening may be due to the influx of Gulf of Aden waters. This circulation pattern causes cross-shelf variations in surface S along the coast, with salinities in coastal waters observed to be up to 2 units lower than corresponding offshore waters (Churchill et al., 2014~~;~~; Sofianos and Johns, 2003~~;~~; Wafar et al., 2016). The implications on the carbonate system of this circulation pattern have not been characterized. This possibly obscures ecosystem-driven perturbations of rTA and rDIC at coral reefs but has only a small effect on the large ecosystem-driven perturbations observed at mangrove forests and seagrass meadows.

By comparing relative changes in rTA and rDIC in each habitat, inferences can be made regarding the balance of ecosystem processes within Red Sea coastal habitats (Figure 8, ~~(~~Albright et al., 2013~~;~~; Challener et al., 2016~~;~~; Cyronak et al., 2018~~;~~; Gattuso et al., 1998~~;~~; Zeebe and Wolf-Gladrow, 2001). If a habitat conforms closely to a linear ~~trend~~relationship, it can be inferred that the balance of ecosystem processes is relatively uniform across sites. The slope of the ~~trend~~ linear relationship indicates the balance of ecosystem processes, with a value determined by the relative proportions of dominant ecosystem processes represented as directional vectors in Figure 8a. Additionally, the intercepts of the linear ~~trend~~ relationship are inherited from the signals of upstream ecosystems, and the amplitude of an observation along this ~~trend~~ linear relationship is an indication of a combination of metabolic rate and residence time. It also follows that if a habitat doesn't conform closely to a linear ~~trend~~relationship, then the balance of ecosystem processes is variable across sites. These inferences can be made from changes in DIC and TA as they are affected by only mixing and metabolic processes and are invariant with temperature or pressure. In contrast, ~~OCP's~~other carbon parameters are all affected strongly by temperature variations and they respond non-linearly to mixing and variations in TA and DIC. Particularly, large but linked changes in TA and DIC in the ratio of roughly 1:1 causes ~~OCP's~~other carbon parameters to change very little (Zeebe and Wolf-Gladrow, 2001). This effect can be observed at the seagrass meadow time series station, with the loss of seasonal cycle in ~~OCP's~~other carbon parameters (Figure 7~~6~~).

All mangrove forests in the Red Sea are comprised of a single species, *Avicennia marina* (~~Chaidez~~ Almahasheer et al. 2016~~et al., 2017~~)~~,~~ and display a relatively uniform balance of ecosystem processes across the Red Sea (Figure 8). Both the time-series data and the spatial data show statistically similar ~~trends~~ linear relationships (Figure 8, Table 1). It follows from this that differences in residence times and metabolic rates are the strongest driver of variability between sites, whilst underlying ecosystem processes remain relatively stable. The positive changes in rTA and rDIC are indicative of high respiration rates, mainly due to high rates of organic matter remineralization, from sediments rich in organic carbon. This lowers pH inducing calcium carbonate dissolution, a mechanism which has been found to be important in previous process-based studies (Burdige & Zimmerman, 2002~~;~~; Krumins et al., 2013; Meister, 2013; Middelburg et al., 1996). Changes in the negative direction, with deficits in rTA and rDIC, are less expected in mangrove forests, as sediments are rarely net autotrophic (Bouillon et al., 2008~~;~~; Krumins et al., 2013~~;~~; Zablocki et al., 2011), but could be inherited from upstream seagrass meadows and coral reefs (Guannel et al., 2016). More support for the latter can be found in time-series observations, with TA and DIC at the mangrove forest station conforming closely to those at the seagrass meadow station, but also displaying erratic deviations towards high rTA and rDIC that varies similarly to other mangrove forest sites (Figure 7~~; Figure~~-8~~ 8~~). A negative rTA intercept is observed in the mangrove forests linear relationship between ~~-~~rTA and ~~:~~rDIC ~~trend~~ (Figure 8), which is consistent with a basin-wide cumulative cross-shelf calcification signal, inherited from upstream coral reefs and potentially even seagrass meadows.

These results suggest that the carbonate system and contributions to air-sea CO_2 exchanges of overlying waters in Red Sea mangrove forests is likely significantly mediated by water residence time and mixing, not only by metabolic rates. The inland mangrove forest sampled contained drastically higher TA and DIC in surrounding waters, and further resulted in higher pCO_2 and a large CO_2 source to the atmosphere, compared to coastally-residing mangrove forests (Figure ~~S2~~S2-3~~, Figure 5~~). De-gassing of CO_2, an increase in calcium carbonate dissolution due to decrease in pH, or an increase in redox processes due to oxygen depletion is most-likely the cause for the ratio of rTA:rDIC deviating at this site to an almost perfect 1:1 ratio, from the 0.61 observed elsewhere. This implies that the carbonate system in stagnant water columns over mangrove forests could be different to what is observed in those with variable water exchanges, and the flushing of mangrove forests from surrounding waters can vastly reduce their contribution to air-sea CO_2 exchanges. As such, the control of surrounding water exchanges and water residence times should be considered further in these ecosystems, as studies often quantify the influence of mangrove forests on air-sea CO_2 exchange using stagnant water columns (Bouillon et al., 2007~~;~~; Bouillon et al., 2008; ~~;~~Macklin et al., 2019~~;~~; Sea et al., 2018).

Red Sea seagrass meadows have a high species diversity (Qurban et al., 2019~~;~~; Kenworthy et al., 2007) and show large ecosystem-driven anomalies in rTA and rDIC, but vary in the balance of ecosystem processes between sites (Figure 8). At the time-series station, a slope of 0.73 is observed, whilst across other sites no ~~significant~~ strong ~~trend linear~~ relationship is found. This slope is consistent with the coupling of photosynthesis and sedimentary calcification, promoted by increased pH due to net autrophy in seagrass meadows, which has been shown to result in a ratio of 1:1 change in rTA:rDIC (Barrón et al., 2006~~;~~; Burdige and Zimmerman, 2002~~;~~; Krumins et al., 2013~~;~~; Lyons et al., 2004~~;~~; Macreadie et al., 2017~~;~~; Unsworth et al., 2012). Sedimentary sulphur and iron oxidation which, occur alongside sedimentary calcification in oxygenated environments and higher pH, potentially contributes to the lowering of the rTA:rDIC slope below 1 (Burdige and Zimmerman, 2002~~;~~; Krumins et al., 2013), however, Red Sea seagrass sediments have been observed to contain low levels of iron (Saderne et al. in review; Anton et al. 2018). At the time-series station, lower TA and DIC in summer months is due to a combination of increased metabolic rates and/or residence times. The variability between rTA and rDIC between sites, and the lack of a significant~~ trend~~ linear relationship indicates that the balance between ecosystem processes is important in driving the carbonate system of Red Sea seagrass meadows, in combination with metabolic rates and residence times. This is a finding that has been confirmed in separate studies, with the balance of ecosystem processes often effected by variable seagrass meadow density and site oxygenation (Burdige and Zimmerman, 2002~~;~~; Krumins et al., 2013~~;~~; Unsworth et al., 2012). Indeed, ~~a separate study of~~ some seagrass meadow sites visited in the present study ~~found that metabolic rates were observed to be~~have highly variable and species dependent metabolic rates (Anton et al. in ~~prep~~review).

Due to small perturbations in the carbonate system exhibited by transition waters and coral reefs and the uncertainty limits of our model, little can be concluded about the large-scale variability in ecosystem processes in ~~this~~ these habitats. Transition waters show few occurrences of ecosystem anomalies inherited from surrounding coastal habitats. Small temporal variations in rTA and rDIC at the coral reef time series station show no ~~trend~~ linear relationship or seasonal cycle, consistent with variability driven by exchanges through the complex reef system rather than inherent ecosystem processes and metabolic rate. Spatial variability shows similar characteristics, which can be attributed to a combination of spatial changes in ecosystem processes, residence times, metabolic rates and connectivity (Cyronak et al., 2018~~;~~; Gattuso et al., 1999; Kleypas et al., 2011~~;~~; Takeshita et al., 2018). What can be concluded is that coral reef and transition waters have little consequence to air-sea carbon fluxes on a local scale, offering little change in the carbonate system compared to offshore conditions (Figure ~~3~~4~~,~~; Figure 6).

The results reported here can offer further explanations to the decadal changes in calcification rates in the Red Sea reported by Steiner et al. (2018), which are also supported within this study (Figure 3). Steiner et al. (2018), reported a 26 ± 16% decline in total $CaCO_3$ deposition rate along the basin between 1998 and 2018, concentrated in the southern Red Sea, suggesting that coral reefs in the southern Red Sea are under stress. Indeed, warming of the Red Sea, which has been faster than the global average (Chaidez et al. 2017), has been reported to reduce coral growth rates (Cantin et al. 2010), and massive bleaching of Red Sea corals south of 20ºN in the summer of 2015 (Hughes et al. 2018, Osman et al. 2018), and replacement by algal turf, may have reduced carbonate deposition rates in the southern Red Sea further. Our analysis suggests additional contributions to decline carbonate deposition in the Red Sea. In particular, mangrove habitats are characterized here as important sites of TA input, likely driven by carbonate dissolution. Hence, the 13% increase in mangrove forests in the Red Sea over the past 30 years (Almahasheer et al. 2016), could also be reflected in increased rates of carbonate dissolution basin-wide.

5. Conclusion

We observed strong evidence of ecosystem-driven perturbations in the carbonate system over Red Sea coastal habitats. We employed a simple single-end-member mixing model to estimate the expected conservative behaviour over the coastal zone of the Red Sea. We find that 1) along-shelf changes in TA and DIC exhibit strong linear ~~trends~~ relationships that are consistent with net basin-scale calcium carbonate precipitation; 2) ecosystem-driven changes in TA and DIC are larger than offshore variations in >~~85~~70% of sampled seagrass meadows and mangrove forests, changes which are influenced by a combination of longer water residence times and community metabolic rates; and 3) the sampled mangrove forests show strong and consistent contributions from both organic respiration and other sedimentary processes (carbonate dissolution and secondary redox processes), while seagrass meadows display more variability in the relative contributions of photosynthesis and other sedimentary processes (carbonate precipitation and oxidative processes). With the available data we cannot conclude if differences in magnitude of rTA and rDIC within habitats reflect differences in residence times or metabolic rates. The results of this study highlight the importance of resolving the influences of water residence times, mixing and upstream habitats on mediating the carbonate system and coastal air-sea CO_2 fluxes over coastal habitats in the Red Sea.

Code Availability

Code for the calculation of the Wilcox Robust ANOVA post-hoc test can be found in the supplementary material. All other code relating to figures and analysis was constructed in R (version 3.4.3) and is available upon request to the corresponding author.

Data Availability

The full data set used in this study can be obtained from PANGAEA (doi: 10.1594/PANGAEA.899850).

Author Contribution

K.B. collected a portion of the KAUST samples, performed most of the sample analysis on KAUST samples, performed data analysis, developed conceptual ideas and wrote the manuscript. V.S. collected a portion of the KAUST samples, performed some sample analysis on KAUST samples and contributed to manuscript preparation. D.C.M. and J.H.C. collected and analysed WHOI samples and contributed to concept development and manuscript preparation. S.A. facilitated the collection of samples at three time series stations. C.M.D contributed to the concept development and ~~aided in~~to manuscript preparation.

Competing Interests

The authors of this manuscript declare no competing interests.

Acknowledgments

This research was funded by King Abdullah University of Science and Technology (KAUST) through baseline funding and competitive center funding to Carlos M. Duarte, and Susana Agusti (BAS/1/1072-01-01). The sample collection and laboratory analysis of KAUST observations was carried out by K. Baldry and V. Saderne. The sample collection and laboratory analysis of Woods Hole Oceanographic Institution (WHOI) observations was supported by Award Nos. USA-00002, KSA-00011 and KSA-00011/02 made by KAUST to WHOI. We thank all of the contributors who were responsible for collecting and managing Red Sea data that was openly sourced. The full data set used in this study can be obtained from PANGAEA (doi: 10.1594/PANGAEA.899850). Supplementary tables and figures can be found in the supporting information accompanying this manuscript. We thank A. K. Gusti, A. Anton, M.L. Berumen, P. Carrillo-de-Albornoz, D.J. Cocker, N. Garcias-Bonet, C.K. Martin, J. Martinez-Ayala and S. Overmans for their help and support in sample collection and CTD deployments towards this study. Finally, we thank Z. Steiner and an anonymous reviewer for their useful comments that contributed to the development of the manuscript.

References

Albright, R., Langdon, C., and Anthony, K.: Dynamics of seawater carbonate chemistry, production, and calcification of a coral reef flat, central Great Barrier Reef, Biogeosciences, 10(10), 6747-6758, doi:10.5194/bg-10-6747-2013, 2013.

Almahasheer, H., Aljowair, A., Duarte, C.M. and Irigoien, X.: Decadal stability of Red Sea mangroves, Estuarine, Coastal and Shelf Science, 169, 164-172, doi: 10.1016/j.ecss.2015.11.027, 2016.

Anderson, L., and Dyrssen, D.: Alkalinity and total carbonate in the Arabian Sea. Carbonate depletion in the Red Sea and Persian Gulf, Marine chemistry, 47(3-4), 195-202, doi:10.1016/0304-4203(94)90019-1, 1994.

Anton, A., Baldry, K., Coker, D., and Duarte, C.M.: ~~Drivers~~ Thermal optima and drivers of the low meetabolic rates of seagrass meadows in the Red Sea, Frontiers in Marine Science, in ~~prep~~review.

Barrón, C., Duarte, C. M., Frankignoulle, M., and Borges, A. V.: Organic carbon metabolism and carbonate dynamics in a Mediterranean seagrass (Posidonia oceanica), meadow, Estuaries and Coasts, 29(3), 417-426, doi:10.1007/BF02784990, 2006.

Bauer, J. E., Cai, W.-J., Raymond, P. A., Bianchi, T. S., Hopkinson, C. S., and Regnier, P. A.: The changing carbon cycle of the coastal ocean, Nature, 504(7478), 61, doi:10.1038/nature12857, 2013.

Bouillon, S., Middelburg, J. J., Dehairs, F., Borges, A. V., Abril, G., Flindt, M. R., Ulomi, S., and Kristensen, E.: Importance of intertidal sediment processes and porewater exchange on the water column biogeochemistry in a pristine mangrove creek (Ras Dege, Tanzania), Biogeosciences, 4(1), 311-322, doi:10.5194/bg-4-311-2007, 2007.

Bouillon, S., Borges, A. V., Castañeda-Moya, E., Diele, K., Dittmar, T., Duke, N. C., Kristensen, E., Lee, S. Y., Marchand, C., and Middelburg, J. J.: Mangrove production and carbon sinks: a revision of global budget estimates, Global biogeochemical cycles, 22, GB2013, doi:10.1029/2007GB003052, 2008.

Burdige, D. J., and Zimmerman, R. C.: Impact of sea grass density on carbonate dissolution in Bahamian sediments, Limnology and Oceanography, 47(6), 1751-1763, doi:10.4319/lo.2002.47.6.1751, 2002.

Camp, E. F., Suggett, D. J., Gendron, G., Jompa, J., Manfrino, C., and Smith, D. J.: Mangrove and Seagrass Beds Provide Different Biogeochemical Services for Corals Threatened by Climate Change, Frontiers in Marine Science, 3(52), 1-16, doi:10.3389/fmars.2016.00052, 2016.

Cantin, N. E., Cohen, A. L., Karnauskas, K. B., Tarrant, A. M. & McCorkle, D. C.: Ocean warming slows coral growth in the central Red Sea, Science, 329(5989), 322–325, doi:10.1126/science.1190182, 2010.

Chaidez, V., Dreano, D., Agusti, S., Duarte, C. M., and Hoteit, I.: Decadal trends in Red Sea maximum surface temperature, Scientific Reports, 7(8144), 1-8, doi:10.1038/s41598-017-08146-z, 2017.

Challener, R. C., Robbins, L. L., and McClintock, J. B.: Variability of the carbonate chemistry in a shallow, seagrass-dominated ecosystem: implications for ocean acidification experiments, Marine and Freshwater Research, 67(2), 163-172, doi:10.1071/MF14219, 2016.

Churchill, J. H., Bower, A. S., McCorkle, D. C., and Abualnaja, Y.: The transport of nutrient-rich Indian Ocean water through the Red Sea and into coastal reef systems, Journal of Marine Research, 72(3), 165-181, doi:10.1357/002224014814901994, 2014.

Cook, R. D., and Weisberg, S.: Graphics for assessing the adequacy of regression models, Journal of the American Statistical Association, 92(483), 490-499, doi:10.2307/2965698, 1997.

Cyronak, T., Andersson, A. J., Langdon, C., Albright, R., Bates, N. R., Caldeira, K., Carlton, R., Corredor, J. E., Dunbar, R. B., and Enochs, I.: Taking the metabolic pulse of the world's coral reefs, PloS one, 13(1), e0190872, doi:10.1371/journal.pone.0190872, 2018.

de Vries, A. J., Tyrlis, E., Edry, D., Krichak, S. O., Steil, B., and Lelieveld, J.: Extreme precipitation events in the Middle East: Dynamics of the Active Red Sea Trough, Journal of Geophysical Research: Atmospheres, 118(13), 7087-7108, doi:10.1002/jgrd.50569, 2013.

Dickson, A. G., Sabine, C. L., and Christian, J. R.: Guide to best practices for ocean CO2 measurements, PICED Special Publication 3: IOCCP Report No. 8, Canada, Sidney:North Pacific Marine Science Organization, 2007.

Doney, S. C.: The growing human footprint on coastal and open-ocean biogeochemistry, Science, 328(5985), 1512-1516, doi:10.1126/science.1185198, 2010.

Duarte, C. M., Hendriks, I. E., Moore, T. S., Olsen, Y. S., Steckbauer, A., Ramajo, L., Carstensen, J., Trotter, J. A., and McCulloch, M.: Is ocean acidification an open-ocean syndrome? Understanding anthropogenic impacts on seawater pH, Estuaries and Coasts, 36(2), 221-236, doi:10.1007/s12237-013-9594-3, 2013.

Gattuso, J.-P., Frankignoulle, M., and Wollast, R.: Carbon and Carbonate Metabolism in Coastal Aquatic Ecosystems, Annual Review of Ecology and Systematics, 29, 405-434, doi:10.1146/annurev.ecolsys.29.1.405, 1998.

Gattuso, J.-P., Allemand, D., and Frankignoulle, M.: Photosynthesis and calcification at cellular, organismal and community levels in coral reefs: a review on interactions and control by carbonate chemistry, American zoologist, 39(1), 160-183, doi:10.1093/icb/39.1.160, 1999.

Gattuso, J.-P., Epitalon ,J.-M., Lavigne, H., and Orr, J.: seacarb: Seawater Carbonate Chemistry. R package version 3.2.6, https://CRAN.R-project.org/package=seacarb, 2018

Giraud, X., Le Quéré, C., and Da Cunha, L. C.: Importance of coastal nutrient supply for global ocean biogeochemistry, Global Biogeochemical Cycles, 22(2), GB2025, doi:10.1029/2006GB002717, 2008.

Guannel, G., Arkema, K., Ruggiero, P., and Verutes, G.: The power of three: coral reefs, seagrasses and mangroves protect coastal regions and increase their resilience, PloS one, 11(7), e0158094, doi:10.1371/journal.pone.0158094, 2016.

Hijmans, R.J.: geosphere: Spherical Trigonometry. R package version 1.5-7, https://CRAN.R-project.org/package=geosphere, 2017.

Hughes, T. P., Anderson, K. D., Connolly, S. R., Heron, S. F., Kerry, J. T., Lough, J. M., Baird, A. H., Baum, J. K., Berumen, M. L., Bridge, T. C., Claar, D. C., Eakin, C. M., Gilmour, J. P., Graham, N. A. J., Harrison, H., Hobbs, J.-P. A., Hoey, A. S., Hoogenboom, M., Lowe, R. J., McCulloch, M. T., Pandolfi, J. M., Pratchett, M., Schoepf, V., Torda, G., and Wilson, S. K.: Spatial and temporal patterns of mass bleaching of corals in the Anthropocene, Science, 359(6371), 80–83, doi: 10.1126/science.aan8048, 2018.

Hydes, D., Jiang, Z., Hartman, M., Campbell, J., Pagnani, M., & Kelly-Gerreyn, B.: Surface DIC and TALK measurements along the M/V Pacific Celebes VOS Line during the 2007-2012 cruises, Carbon

Dioxide Information Analysis Center. Oak Ridge National Laboratory, US Department of Energy, Oak Ridge, Tennessee, doi:10.3334/CDIAC/OTG.VOS_PC_2007-2012, 2012.

Jiang, Z. P., Tyrrell, T., Hydes, D. J., Dai, M., and Hartman, S. E.: Variability of alkalinity and the alkalinity-salinity relationship in the tropical and subtropical surface ocean, Global Biogeochemical Cycles, 28(7), 729-742, doi:10.1002/2013GB004678, 2014.

Kenworthy, W. J., Wyllie-Echeverria, S., Coles, R. G., Pergent, G., and Pergent-Martini, C.: Seagrass conservation biology: an interdisciplinary science for protection of the seagrass biome, in: Seagrasses: Biology, Ecology and Conservation, Springer, Dordrecht, 595-623, doi:10.1007/978-1-4020-2983-7_25, 2007.

Kleypas, J. A., Anthony, K. R., and Gattuso, J. P.: Coral reefs modify their seawater carbon chemistry–case study from a barrier reef (M oorea, F rench P olynesia), Global Change Biology, 17(12), 3667-3678, doi:10.1111/j.1365-2486.2011.02530.x, 2011.

Krumgalz, B., Erez, J., and Chen, C.: Anthropogenic CO2 penetration in the northern Red Sea and in the Gulf of Elat (Aqaba), Oceanologica Acta, 13(3), 283-290, 1990.

Krumins, V., Gehlen, M., Arndt, S., Cappellen, P. V., and Regnier, P.: Dissolved inorganic carbon and alkalinity fluxes from coastal marine sediments: model estimates for different shelf environments and sensitivity to global change, Biogeosciences, 10(1), 371-398, doi:10.5194/bg-10-371-2013, 2013.

Lyons, T. W., Walter, L. M., Gellatly, A. M., Martini, A. M., and Blake, R. E.: Sites of anomalous organic remineralization in the carbonate sediments of South Florida, USA: the sulfur cycle and carbonate-associated sulfate, Special Papers-Geological Society of America, 379, 161-176, doi:10.1130/0-8137-2379-5.161, 2004.

Macklin, P. A., Suryaputra, I. G. N. A., Maher, D. T., Murdiyarso, D., and Santos, I. R.: Drivers of CO2 along a mangrove-seagrass transect in a tropical bay: Delayed groundwater seepage and seagrass uptake, Continental Shelf Research, 172, 57-67, doi:10.1016/j.csr.2018.10.008, 2019.

Macreadie, P. I., Serrano, O., Maher, D. T., Duarte, C. M., and Beardall, J.: Addressing calcium carbonate cycling in blue carbon accounting, Limnology and Oceanography Letters, 2(6), 195-201, doi:10.1002/lol2.10052, 2017.

Osman, E.O., Smith, D.J., Ziegler, M., Kürten, B., Conrad, C., El-Haddad, K.M., Voolstra, C.R. and Suggett, D.J.: Thermal refugia against coral bleaching throughout the northern Red Sea, Global change biology, 24(2), e474-e484, doi: 10.1111/gcb.13895, 2018.

Papaud, A., and Poisson, A.: Distribution of dissolved CO2 in the Red Sea and correlations with other geochemical tracers, Journal of marine research, 44(2), 385-402, doi:10.1357/002224086788405347, 1986.

Picheral, M., Searson, S., Taillandier, V., Bricaud, A., Boss, E., Ras, J., Claustre, H., Ouhssain, M., Morin, P., Tremblay, J., Coppola, L., Gattuso, J., Metzl, N., Thuillier, D., Gorsky, G., Tara Oceans Consortium, Coordinators; Tara Oceans Expedition, Participants (2014): Vertical profiles of environmental parameters measured on discrete water samples collected with Niskin bottles during the Tara Oceans expedition 2009-2013. PANGAEA, https://doi.org/10.1594/PANGAEA.836319

Qurban, M. A. B., Karuppasamy, M., Krishnakumar, P. K., Garcias-Bonet, N., and Duarte, C. M.: Seagrass Distribution, Composition and Abundance Along the Saudi Arabian Coast of Red Sea, in: Oceanographic and Biological Aspects of the Red Sea, edited by: Rasul, N. M. A., and Stewart, I. C. F., Springer, Cham, 367-385, doi:10.1007/978-3-319-99417-8_20, 2019.

R Core Team: R: A language and environment for statistical computing, Foundation for Statistical Computing, Vienna, Austria, https://www.R-project.org/, 2017.

Robbins, P. E.: Oceanic carbon transport carried by freshwater divergence: Are salinity normalizations useful?, Journal of Geophysical Research: Oceans, 106(C12), 30939-30946, doi:10.1029/2000JC000451, 2001.

Saderne, V., Baldry, K., Anton, A., Agusti, S., Duarte, C.M.: Characterization of the CO2 system in a coral reef, a seagrass meadow and a mangrove forest in the central Red Sea, Journal of Geophysical Research:Oceans, in review.

Sea, M. A., Garcias-Bonet, N., Saderne, V., and Duarte, C. M.: Carbon dioxide and methane fluxes at the air–sea interface of Red Sea mangroves, 15, 5365-5375, doi:10.5194/bg-15-5365-2018, 2018.

Sofianos, S. S., and Johns, W. E.: An oceanic general circulation model (OGCM) investigation of the Red Sea circulation: 2. Three-dimensional circulation in the Red Sea, Journal of Geophysical Research: Oceans, 108(C3), 3066, doi:10.1029/2001JC001185, 2003.

Steiner, Z., Erez, J., Shemesh, A., Yam, R., Katz, A., and Lazar, B.: Basin-scale estimates of pelagic and coral reef calcification in the Red Sea and Western Indian Ocean, Proceedings of the National Academy of Sciences, 111(46), 16303-16308, doi:10.1073/pnas.1414323111, 2014.

Steiner, Z., Turchyn, A. V., Harpaz, E., and Silverman, J.: Water chemistry reveals a significant decline in coral calcification rates in the southern Red Sea, Nature communications, 9(1), 3615, doi:10.1038/s41467-018-06030-6, 2018.

IPCC: Climate change 2013: The physical science basis: Working Group I contribution to the Fifth assessment report of the Intergovernmental Panel on Climate Change: Cambridge University Press, Cambridge, United Kingdom, doi:10.1017/CBO9781107415324, 2014.

Takeshita, Y. T., Cyronak, T., Martz, T. R., Kindeberg, T., and Andersson, A. J.: Coral reef carbonate chemistry variability at different functional scales, Frontiers in Marine Science, 5, 175, doi:10.3389/fmars.2018.00175, 2018.

Unsworth, R. K., Collier, C. J., Henderson, G. M., and McKenzie, L. J.: Tropical seagrass meadows modify seawater carbon chemistry: implications for coral reefs impacted by ocean acidification, Environmental Research Letters, 7(2), 024026, doi:10.1088/1748-9326/7/2/024026, 2012.

Wafar, M., Ashraf, M., Manikandan, K. P., Qurban, M. A., and Kattan, Y.: Propagation of Gulf of Aden Intermediate Water (GAIW) in the Red Sea during autumn and its importance to biological production, Journal of Marine Systems, 154, 243-251, doi:10.1016/j.jmarsys.2015.10.016, 2016.

Mair, P., and Wilcox, R.: WRS2: Wilcox robust estimation and Testing, R package ver 3.4.4, 2018.

Wurgaft, E., Steiner, Z., Luz, B., and Lazar, B.: Evidence for inorganic precipitation of CaCO3 on suspended solids in the open water of the Red Sea, Marine Chemistry, 186, 145-155, doi:10.1016/j.marchem.2016.09.006, 2016.

Zablocki, J. A., Andersson, A. J., and Bates, N. R.: Diel aquatic CO_2 system dynamics of a Bermudian mangrove environment, Aquatic geochemistry, 17(6), 841, doi:10.1007/s10498-011-9142-3, 2011.

Zeebe, R. E., and Wolf-Gladrow, D. A.: CO_2 in seawater: Equilibrium, kinetics, isotopes, Elsevier Oceanography Series, 65, Elsevier, 1-136, 2001.

Zhan, P., Subramanian, A. C., Yao, F., and Hoteit, I.: Eddies in the Red Sea: A statistical and dynamical study, Journal of Geophysical Research: Oceans, 119(6), 3909-3925, doi:10.1002/2013JC009563, 2014.

Figures

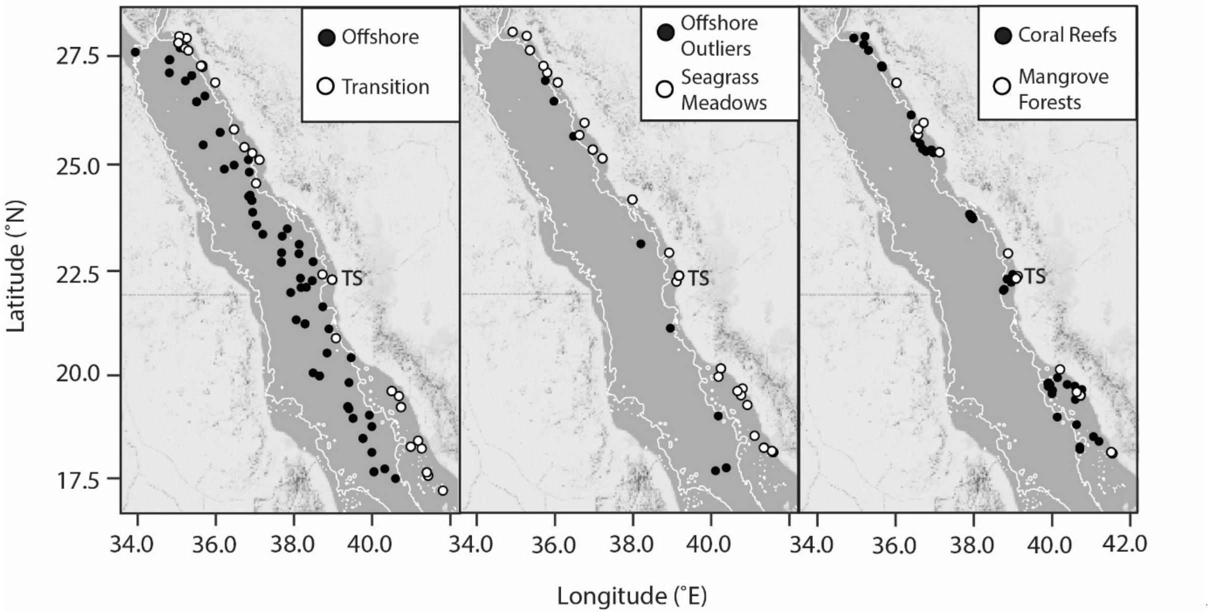

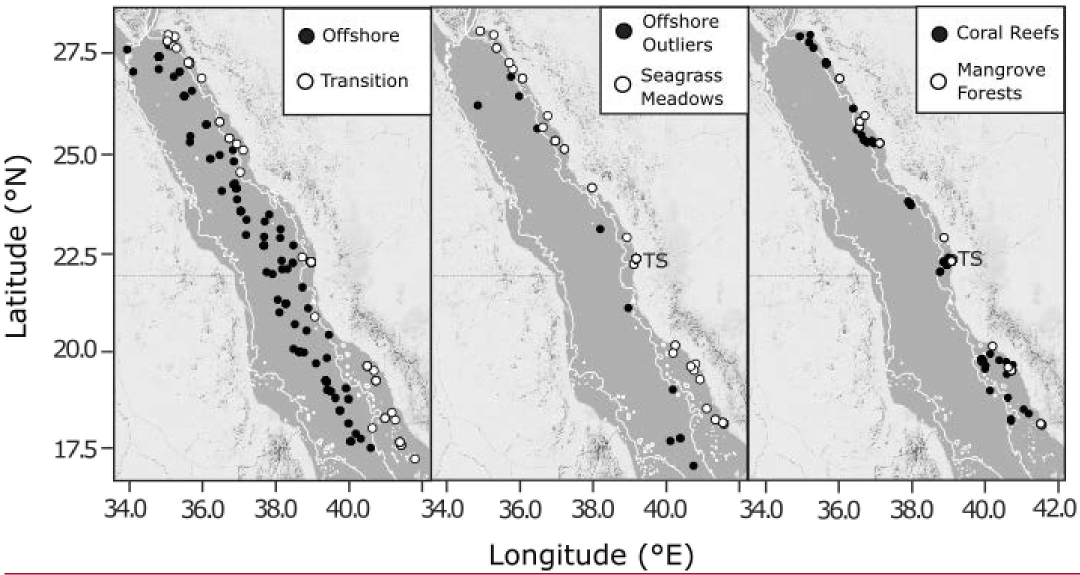

Figure 1. The spatial distribution of combined observations from the Red Sea data sets used in the present study, shown against a 200m bathymetry boundary (thin white line). Observations are classified as offshore, transition, seagrass meadows, coral reefs or mangrove forests. ~~The latitude at which t~~Time series stations are at is indicated ~~by the text "~~as TS (Figure S1)~~"~~. Outliers identified in offshore observations are also shown.

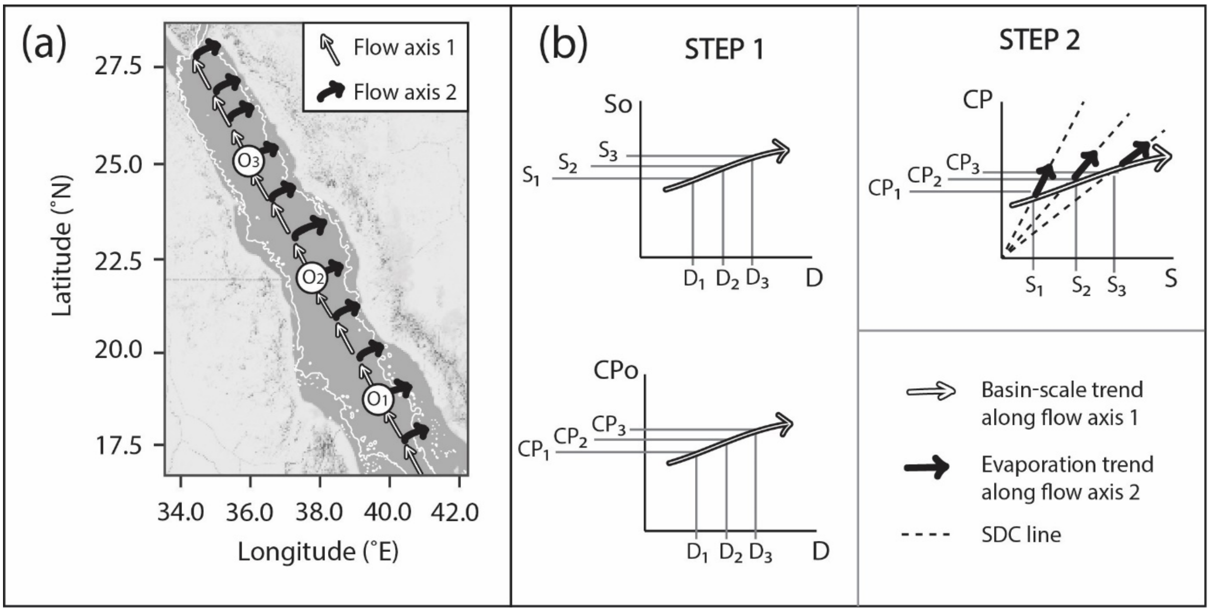

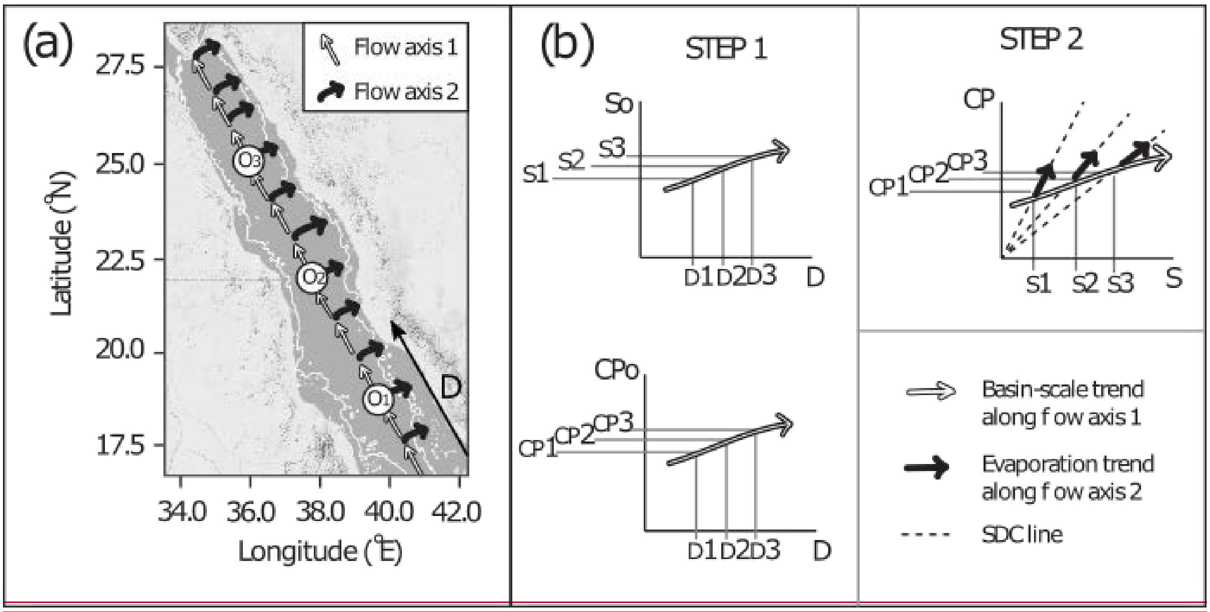

Figure 2. Schematic of the single-end-member mixing model used in the present study. Panel (a) displays the assumed circulation pattern which has two flow axes. Flow axis 1 is along the south-north central axis where waters experience cumulative changes due to basin-scale evaporation and calcification. Flow axis 2 is perpendicular to this axis, where it is assumed that evaporative effects prevail as waters transition from offshore locations (Oi) to coastal regions. The thin white line indicates the 200m bathymetry and the transition from

offshore to coastal waters. Panel (b) explains the single-end-member mixing model in two steps, to ~~estimate~~ determine conservative estimates of a carbon parameter (CP: TA or DIC) for the coastal zone. O_i represents an offshore end-member at a location in ~~the~~ offshore ~~end-member~~waters lying along flow axis 1 (the central axis) at distance D_i,, from a fixed reference point in the southern Resd Sea, and corresponding salinity S_i~~,~~ and carbon parameter measurement ~~of~~ CP_i, as derived from basin~~-~~scale ~~trends~~linear relationships. CP_i is then scaled along the simple dilution and concentration (SDC) line to obtain coastal estimates for carbon parameters.

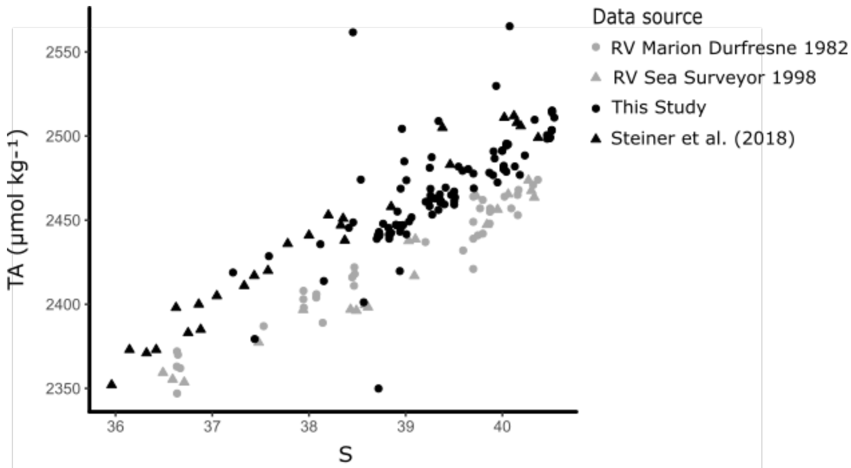

Figure 3. Observations of TA are shown against S, as in Steiner et al. (2018), to illustrate the difference between old (grey) and new (black) observations of carbonate chemistry in the Red Sea.

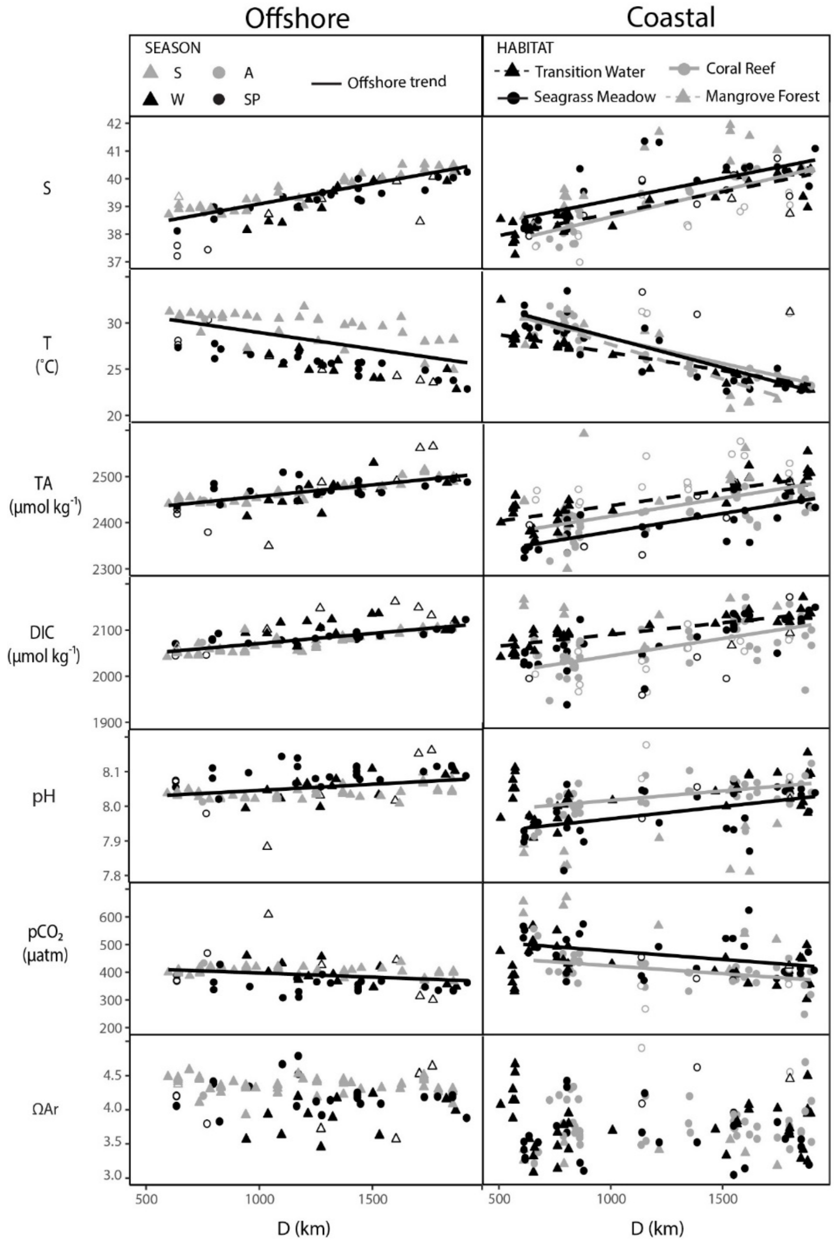

Offshore
Coastal
SEASON
S
A
W
SP
Offshore trend
HABITAT
Transition Water
Coral Reef
Seagrass Meadow
Mangrove Forest
S
T (°C)
TA (µmol kg⁻¹)
DIC (µmol kg⁻¹)
pH
pCO₂ (µatm)
ΩAr
D (km)
D (km)

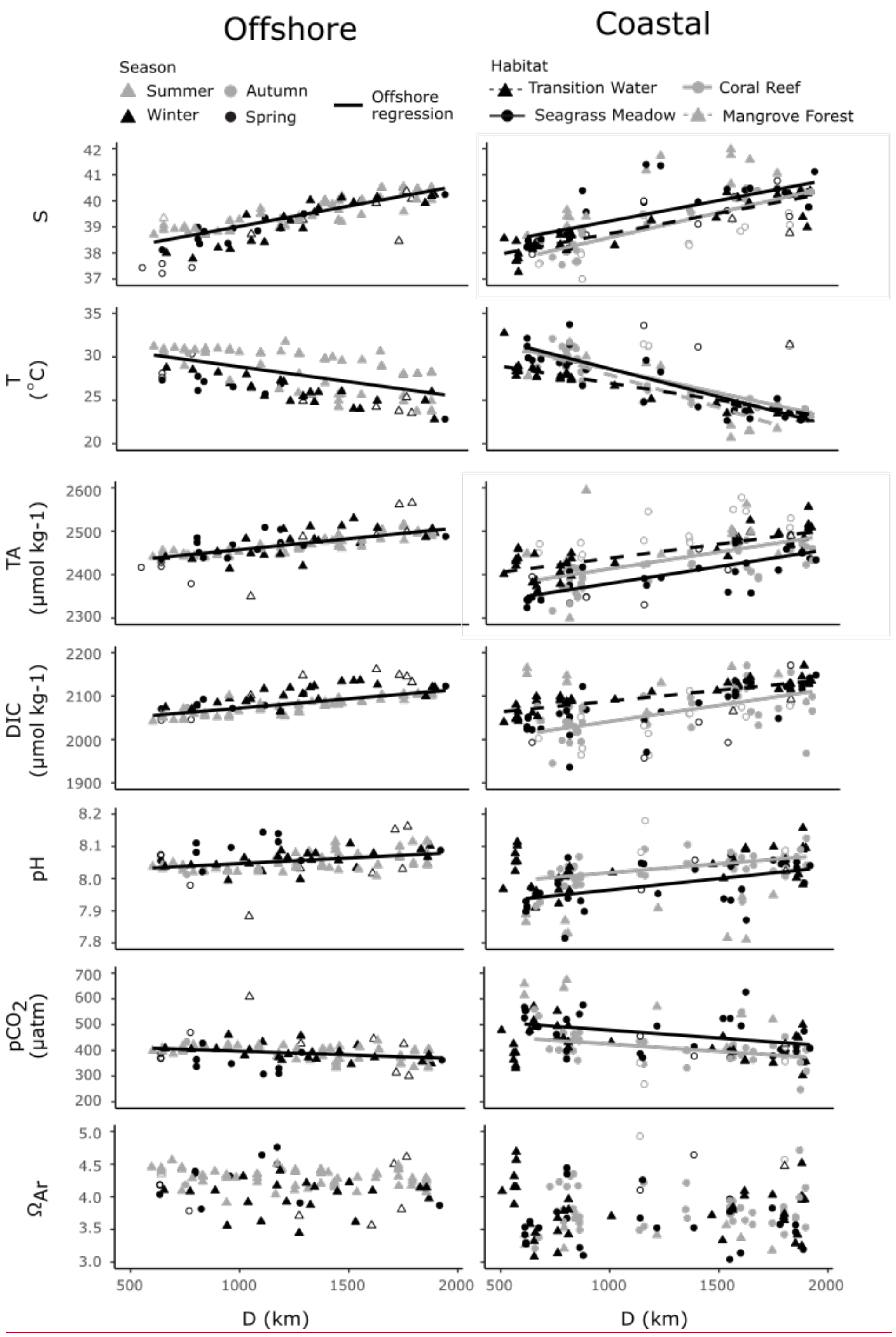

Figure ~~3~~4. Offshore o~~O~~bservations of S, T and carbon variables (left) ~~in the offshore end-member (left)~~ and four coastal habitats (right) are presented against distance along the south-north central axis (D), on the same scales. Significant linear regressions for all combinations of variables are drawn as lines, with associated statistics reported in Table S3. Offshore outliers were not included in determining offshore regressions against D. Coastal observations from time series stations and an outlying mangrove observation were not included in regressions against D. Note that not all coastal observations are displayed, an expanded scale is shown in Figure 6~~5~~. Hollow symbols indicate offshore outliers (right panel) and coastal summer observations (left panel). ~~S = summer, A = autumn, W = winter and SP = spring.~~

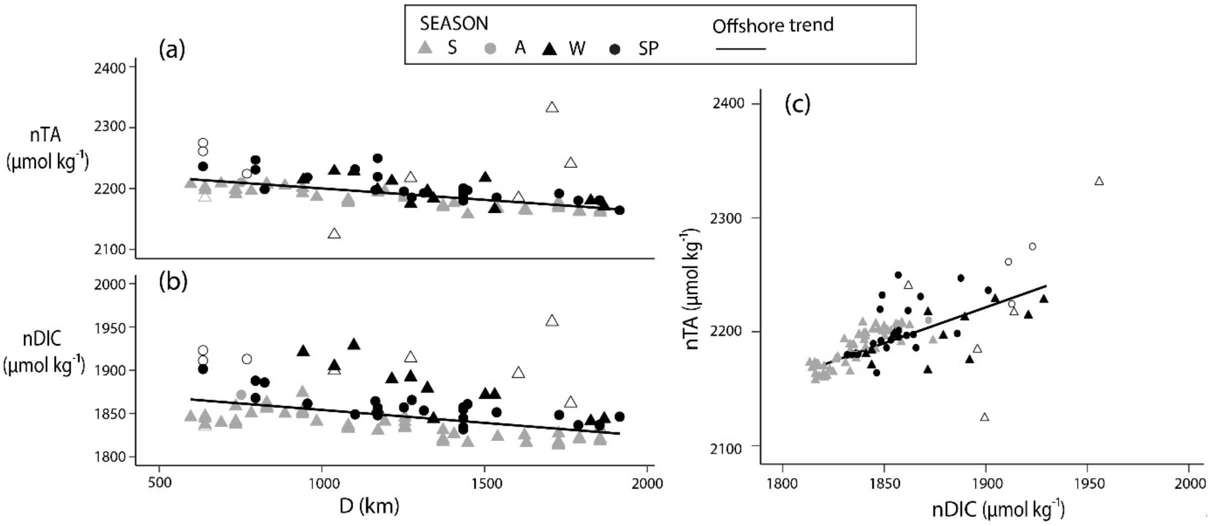

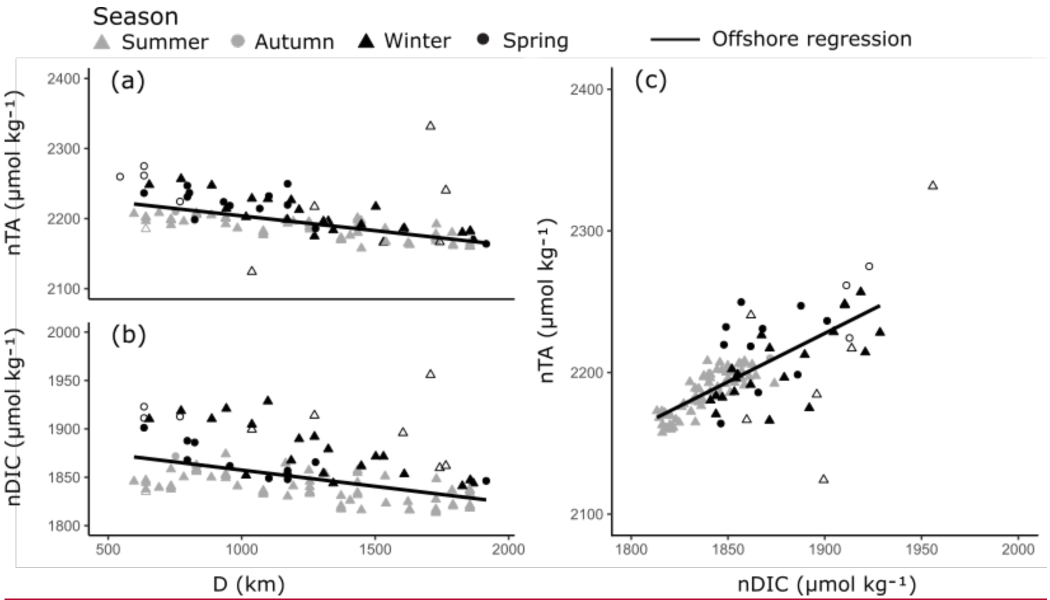

Figure ~~4~~5. Linear relationship~~Trend~~s in nTA and nDIC along the south-north central axis of the Red Sea (a-b), and between nTA and nDIC (c) in the offshore ~~end-member~~waters. Symbols indicate the season in which samples were collected. ~~in:; summer (S), autumn (A), winter (W) or spring (SP).~~ All ~~trends~~ linear relationships were statistically significant and offshore outliers were not included in the linear regressions (hollow symbols).

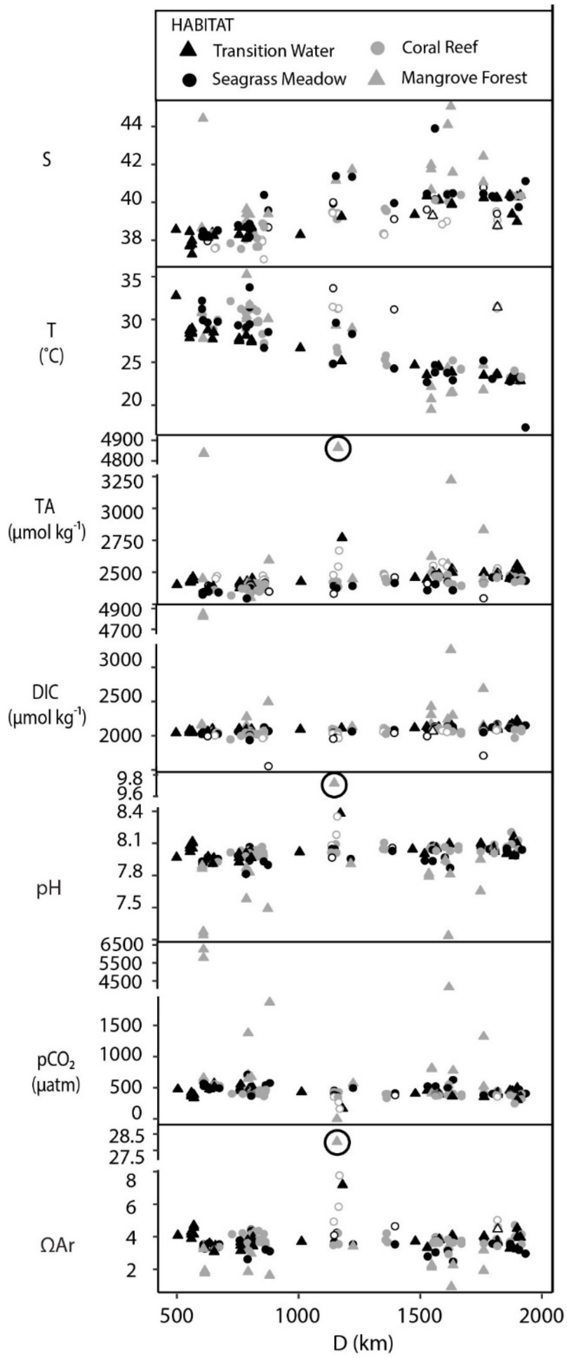

~~**Figure 5.** Observations of S, T and carbon variables at four coastal habitats are presented against distance along the south-north central axis (D) on an expanded scale. The circle indicates the location of one outlying observation, of TA and DIC that produce un-realistic values of OCP's~~other carbon parameters~~. Hollow symbols indicate coastal summer observations.~~

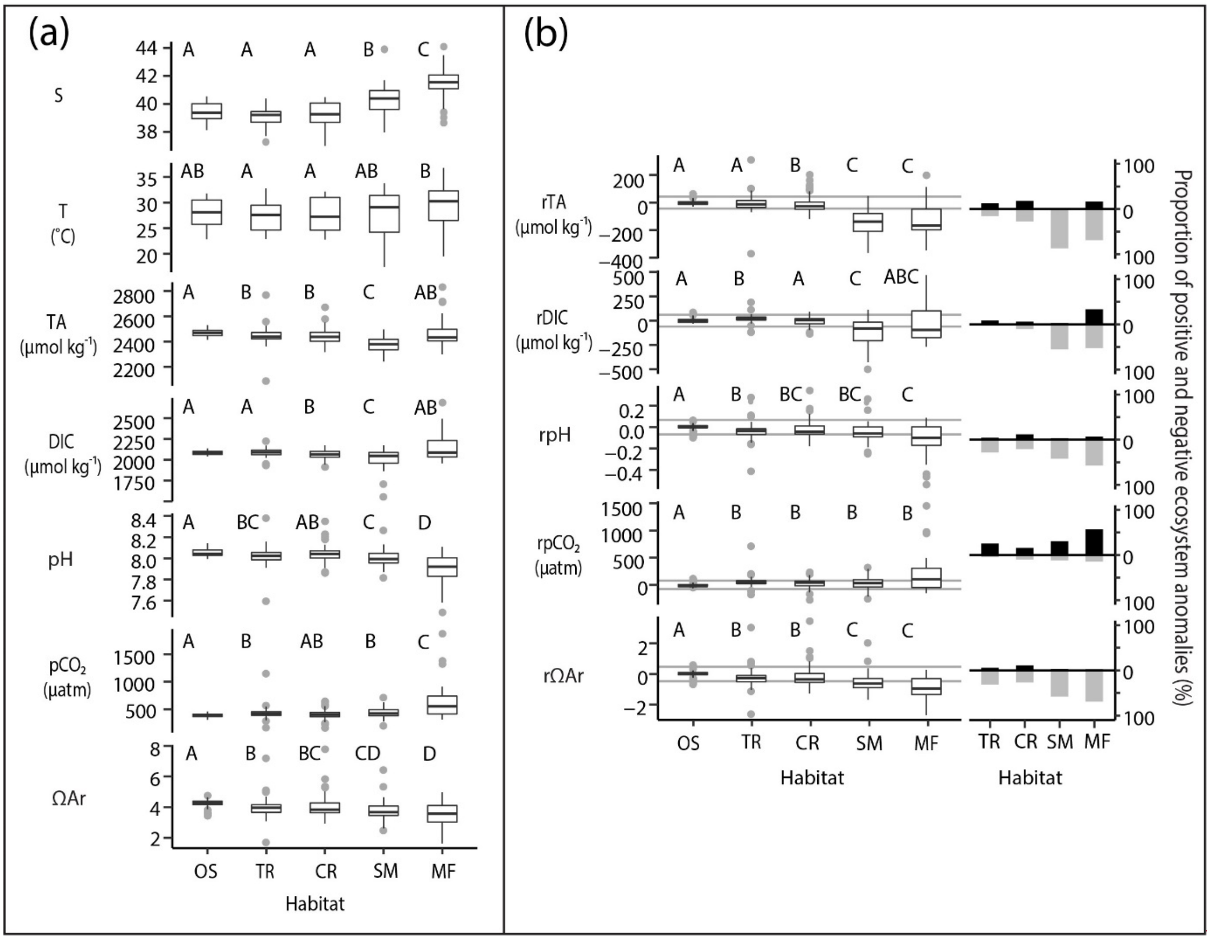
(a)
S
T
(°C)
TA
(µmol kg-1)
DIC
(µmol kg-1)
pH
pCO2
(µatm)
ΩAr
OS
TR
CR
SM
MF
Habitat
(b)
rTA
(µmol kg-1)
rDIC
(µmol kg-1)
rpH
rpCO2
(µatm)
rΩAr
Habitat
Proportion of positive and negative ecosystem anomalies (%)

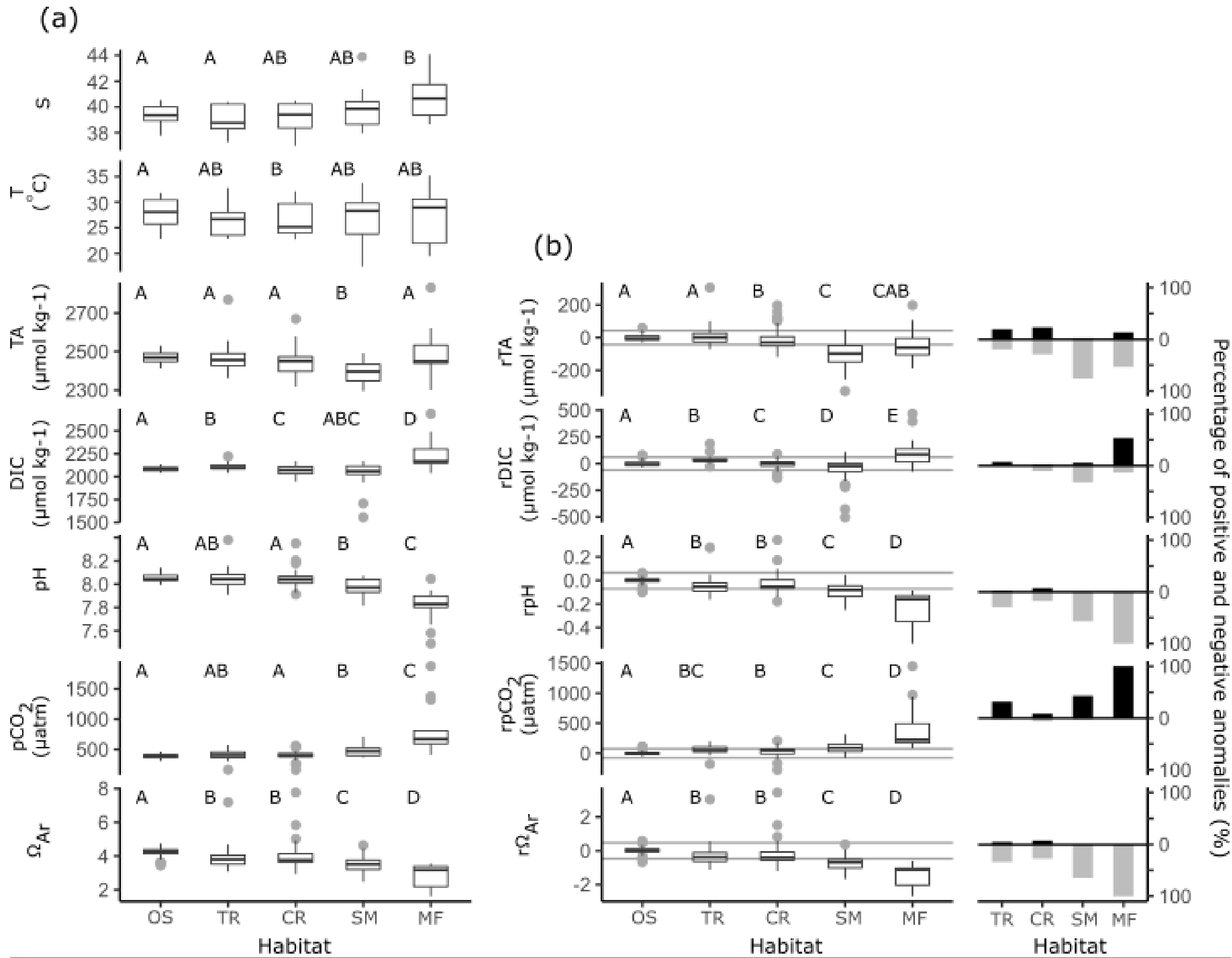

Figure 6~~6~~. Box-plot distributions of (a) observed S, T, carbon variables and (b) non-conservative carbonate system residuals are presented by habitat group:~~;~~ offshore (OS), transition waters (TR), coral reef (CR), seagrass meadow (SM) and mangrove forest (MF). Each box-plot displays the median, the first and third quartiles, and whiskers that extend to the mean +/- 1.5 times the inter-quartile range. Grey dots represent observations that extend outside the whiskers of the boxplot. Grey lines in panel (b) indicate the upper and lower bounds of the 99% P.I. defined by offshore observations. The proportion of ecosystem anomalies (%) observed in both the positive and negative directions are presented alongside, and to the right of boxplots in panel (b) (Table S4). Grouping letters (A-D) assigned above boxplots indicate the results of post-hoc bootstrapped t-tests, summarized from statistics presented in Table S5. If tests showed significant similarities at the 0.05 significance level with another habitat across a variable they were assigned the same letter.

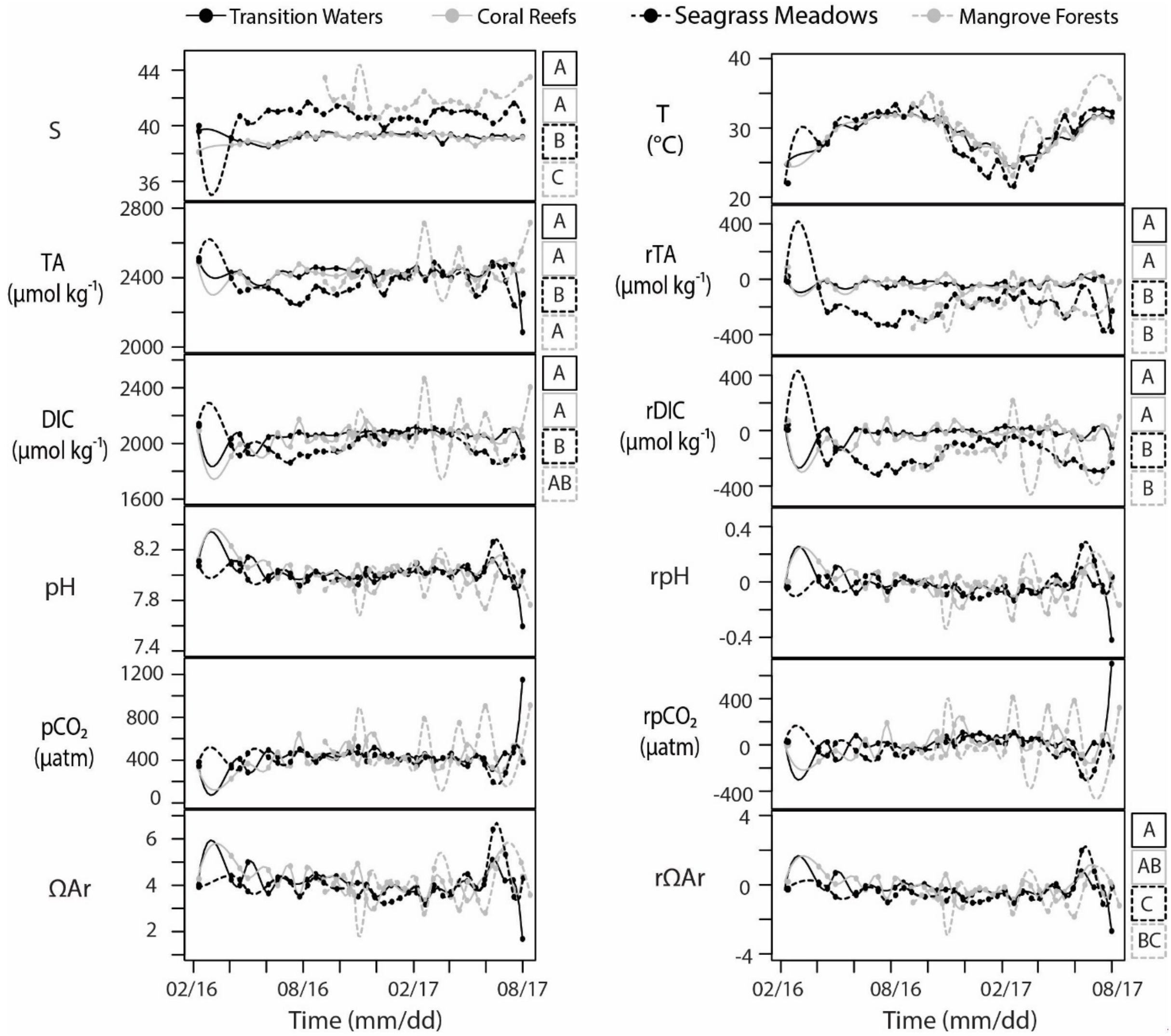

Transition Waters
Coral Reefs
Seagrass Meadows
Mangrove Forests
S
TA (μmol kg-1)
DIC (μmol kg-1)
pH
pCO2 (μatm)
ΩAr
T (°C)
rTA (μmol kg-1)
rDIC (μmol kg-1)
rpH
rpCO2 (μatm)
rΩAr
Time (mm/dd)
02/16
08/16
02/17
08/17

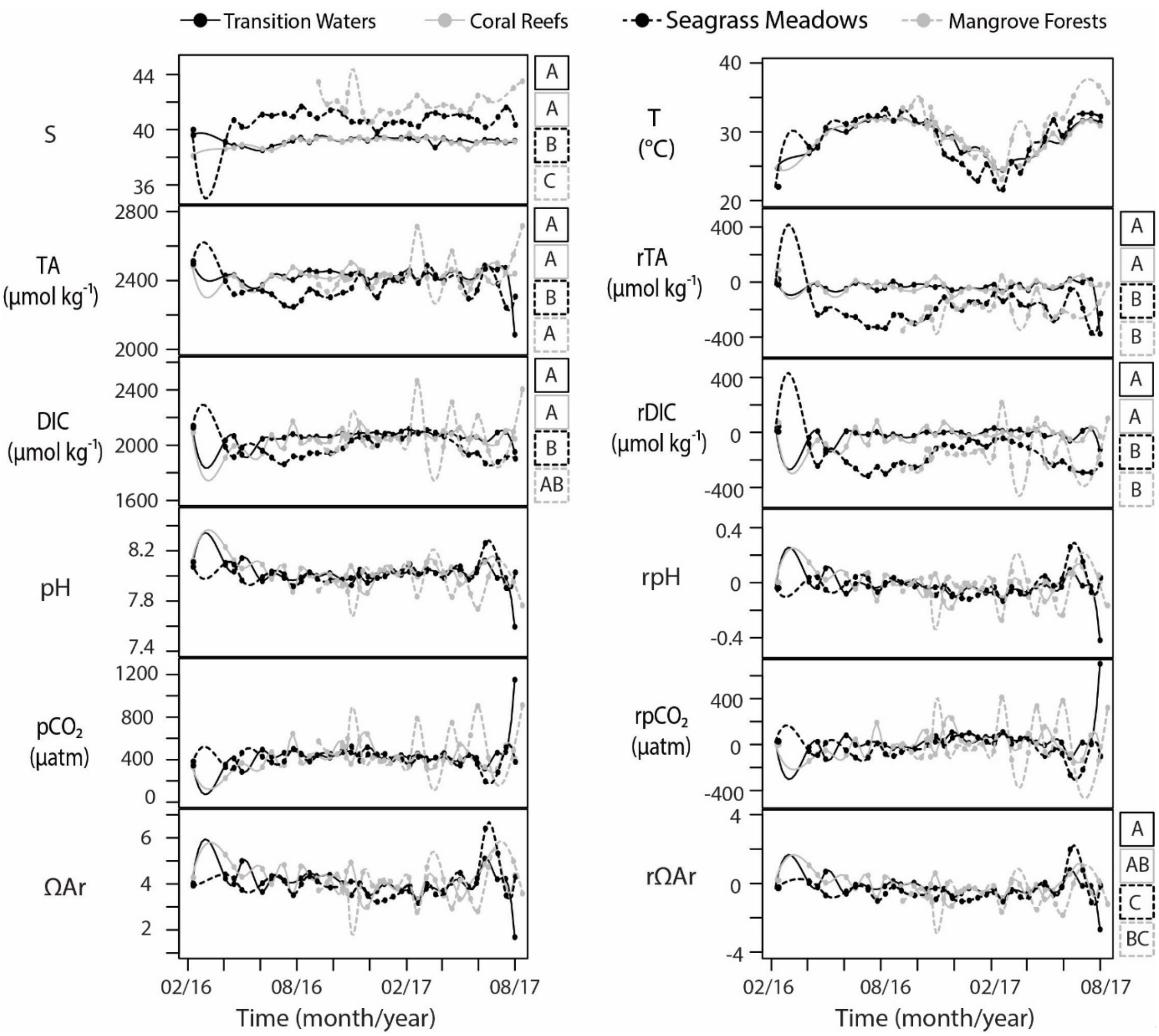
Transition Waters
Coral Reefs
Seagrass Meadows
Mangrove Forests
S
T (°C)
TA (µmol kg-1)
rTA (µmol kg-1)
DIC (µmol kg-1)
rDIC (µmol kg-1)
pH
rpH
pCO2 (µatm)
rpCO2 (µatm)
ΩAr
rΩAr
02/16
08/16
02/17
08/17
Time (month/year)
Time (month/year)

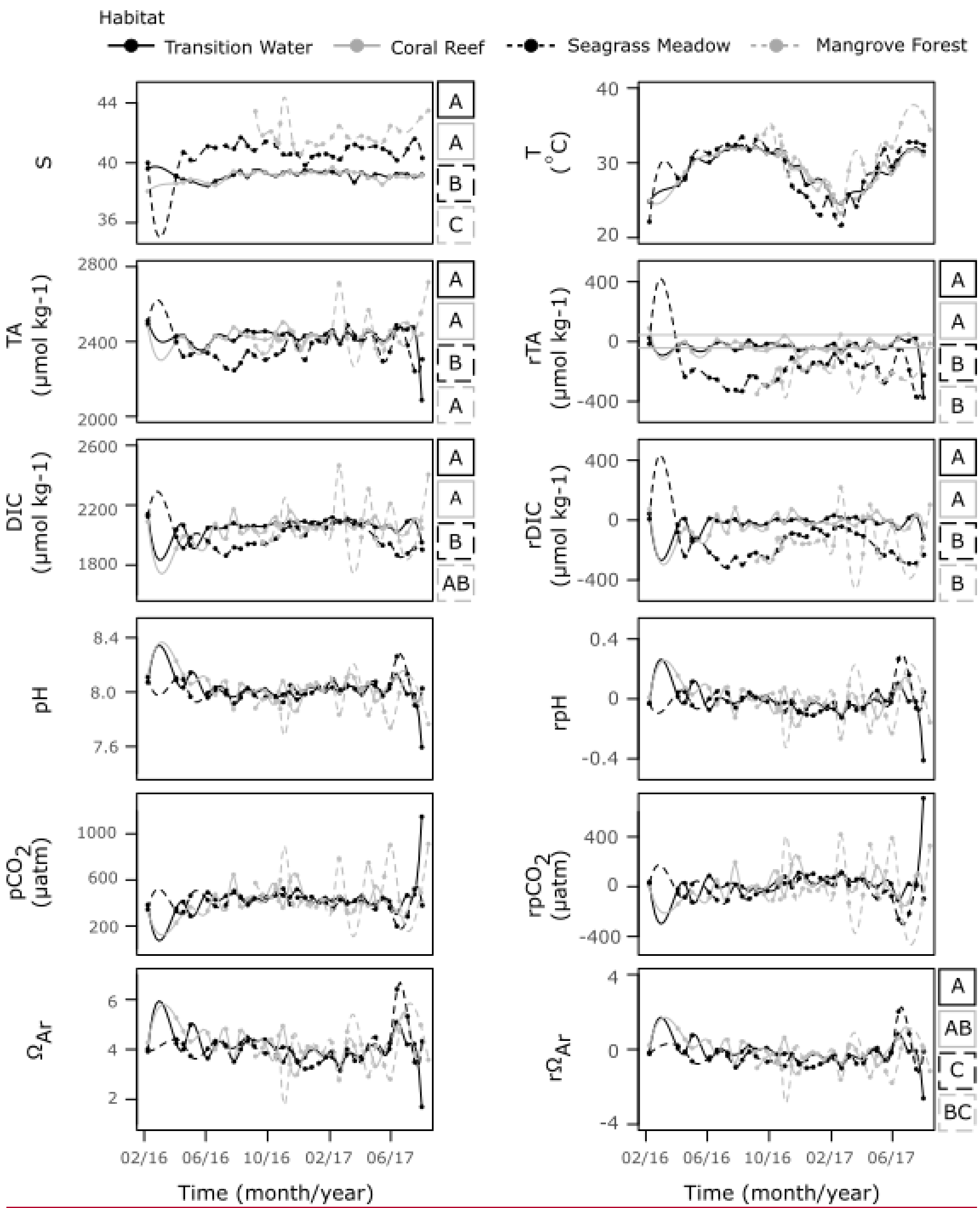

Figure ~~7~~7. Time series observations of S, T, carbon variables and non-conservative carbonate system residuals collected from the four time series stations. Observations are shown fitted with a spline function of order 100 by the method of Forsythe, Malcolm and Moler (1977). For variables which displayed a significant result for WR-ANOVA tests for differences in medians across habitat groups, results from post-hoc bootstrapped t-tests are shown as letters (A-C) to the right of the plot. If tests showed significant similarities at the 0.05 significance level with another habitat across a variable they were assigned the same letter.

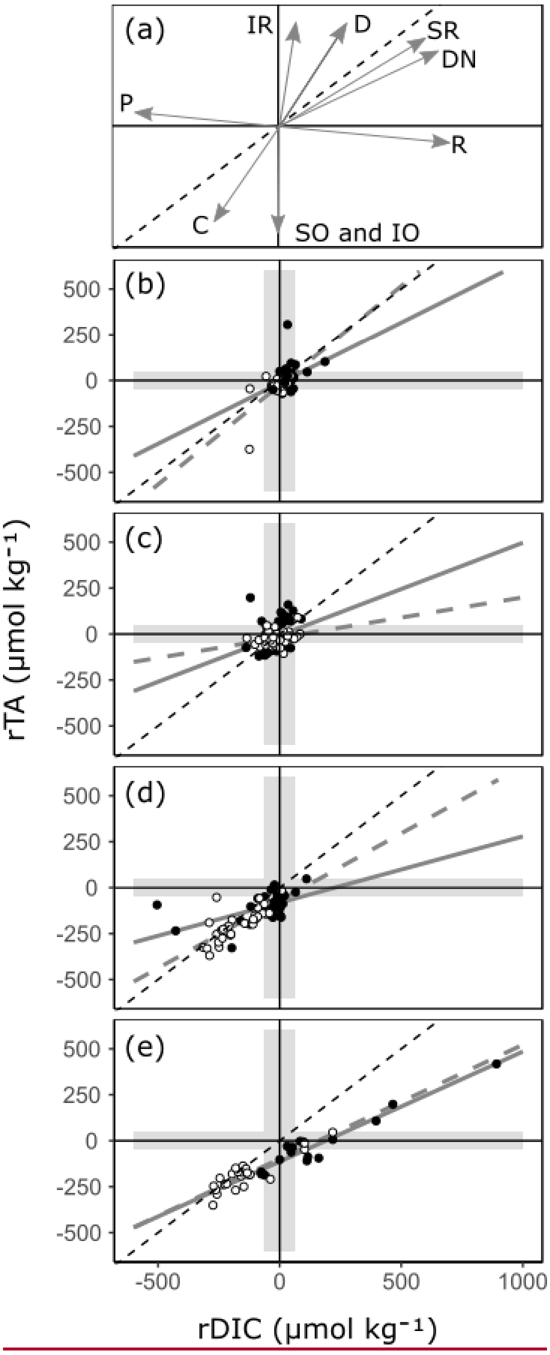

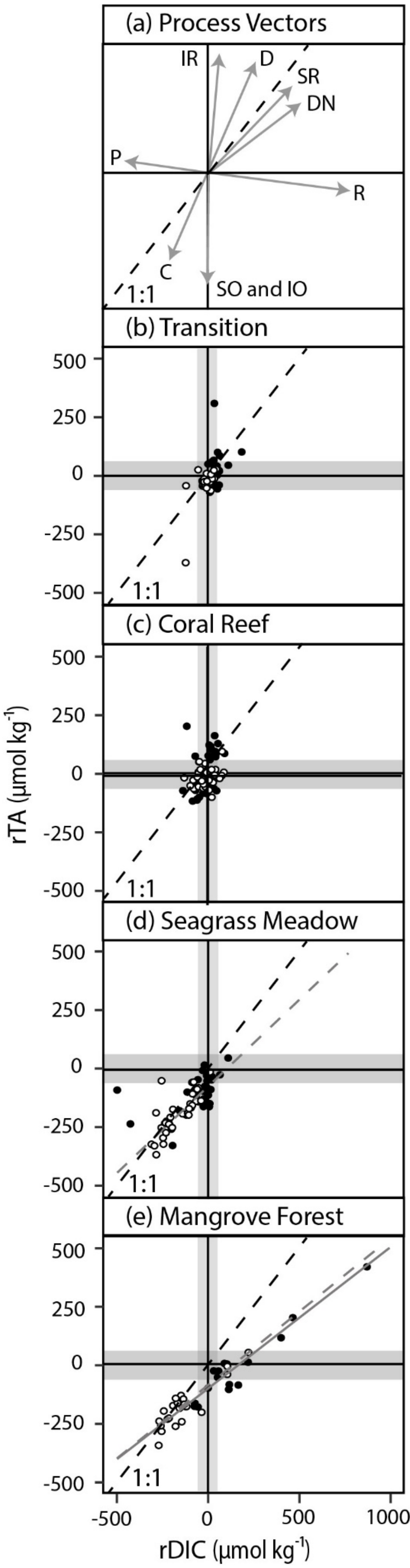

Figure ~~8~~8. A reference plot (a) showing unitless directional vectors of change in the rTA vs. rDIC space for multiple ecosystem processes. Below, observations of rTA vs. and rDIC from transition water and the three coastal habitats is presented~~.~~: (b) transition water, (c) coral reef, (d) seagrass meadow and (e) mangrove forest~~(b-e)~~. Time series observations are indicated with open circles, and all other spatial data is indicated with closed circles. A 1:1 reference line is shown in all plots (black dashed line) as well as regression lines ($r^2 > 0.6$) for the time series subset (grey dashed line) and the spatial subset (grey solid line). The reference plot includes directional vectors for calcium carbonate precipitation (C), calcium carbonate dissolution (D), primary production (P), respiration (R), iron reduction (IR), sulphate reduction (SR), denitrification (DN), sulphur oxidation (SO) and iron oxidation (IO). The shaded envelope represents the calculates 99% P.I. for rTA and rDIC. An expanded figure of panel (e) showing inland mangrove stands is presented in Figure S2b.

Tables

Table 1: Intercept (±SE), slope (±SE), correlation coefficient (r^2), F statistics (F) and p-values (p) of linear regressions of rTA versus rDIC for different subsets of coastal observations.

Data subset	**Intercept**	**Slope**	**r^2**	**F**	**p**
Transition Water	-24.~~7~~6 (±7.~~8~~5)	0.~~90~~91 (±0.17)	0.~~28~~29	27.~~2~~8	<0.001
Coral Reef	-~~9.8~~11.3 (±6.1)	0.39 (±0.13)	0.08	8.~~47~~55	0.004
Seagrass Meadow: Times-series	-~~70~~71.~~9~~4 (±20.~~5~~8)	0.73 (±0.11)	0.60	45.~~21~~26	<0.001
Seagrass Meadow: Spatial	-~~80~~81.~~2~~9 (±12.~~2~~4)	0.36 (±0.09)	0.32	15.~~7~~8	<0.001
Mangrove Forest: Time-series	-98.7 (±13.2)	0.62 (±0.07)	0.79	77.26	<0.001
Mangrove Forest: Spatial	-~~112~~113.2.~~2~~ (±~~13.58~~13.4)	0.~~60~~60 (±0.~~05~~05) (0.86 with inland stands)	0.92	~~159.8~~161.8	<0.001

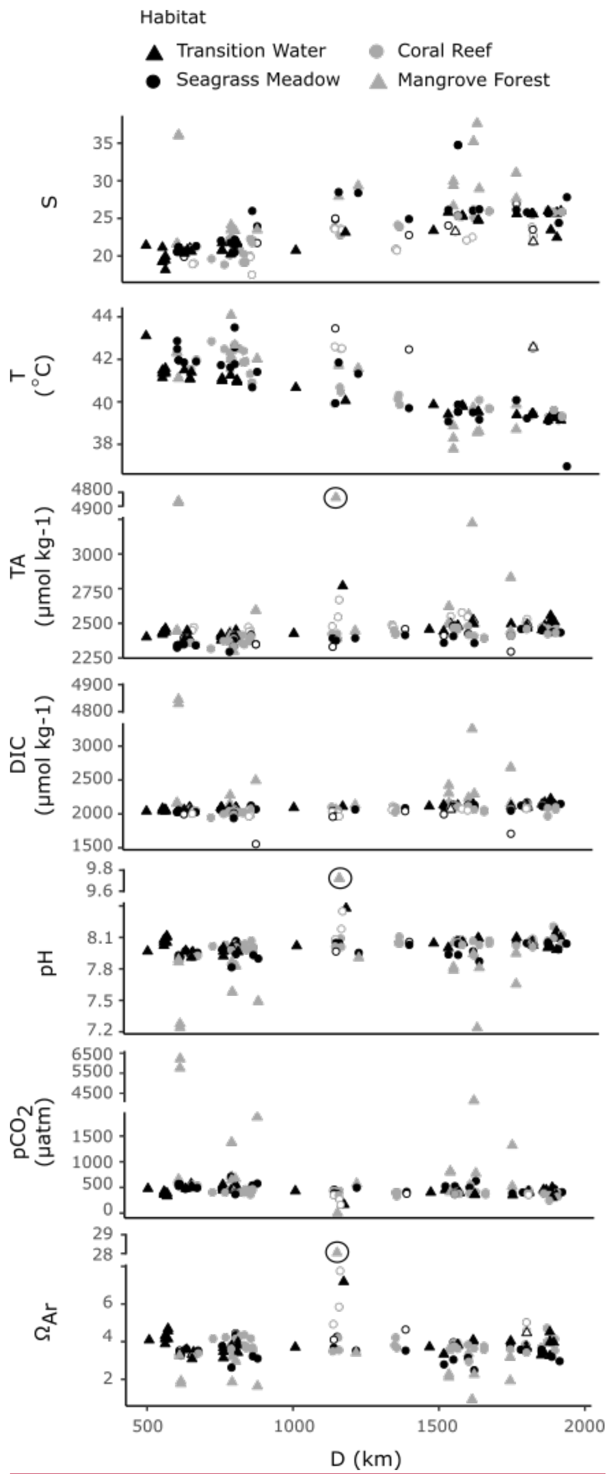

Figure S2. Observations of S, T and carbon variables at four coastal habitats are presented against distance along the south-north central axis (D) on an expanded scale. The circle indicates the location of one outlying mangrove forest observation of TA and DIC that produces un-realistic values of other carbon parameters. Note that observations from time series stations are excluded. Hollow symbols indicate coastal summer observations.

Marked up supplementary material

Supplementary Information:

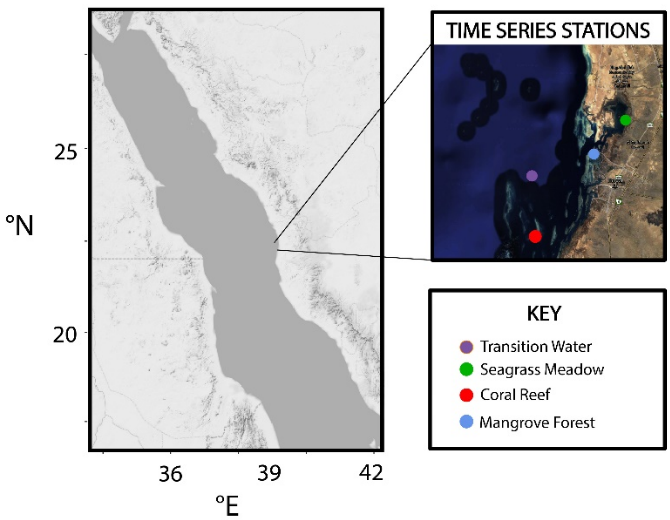

Figure S1: Positions of the four time series stations

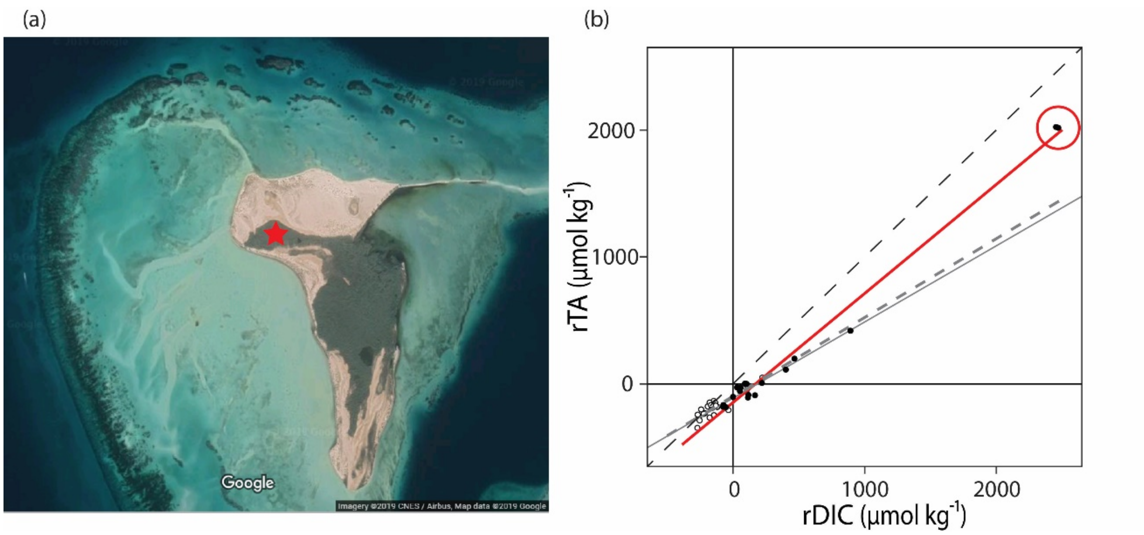
(a)
Google
Imagery ©2019 CNES / Airbus, Map data ©2019 Google
(b)
2000
1000
0
rTA (μmol kg-1)
0
1000
2000
rDIC (μmol kg-1)

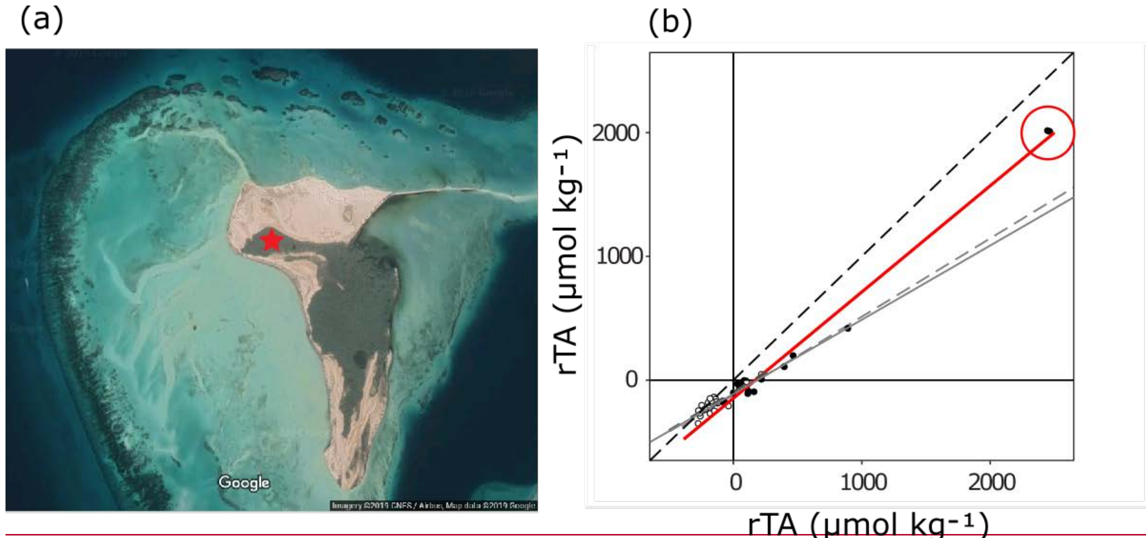

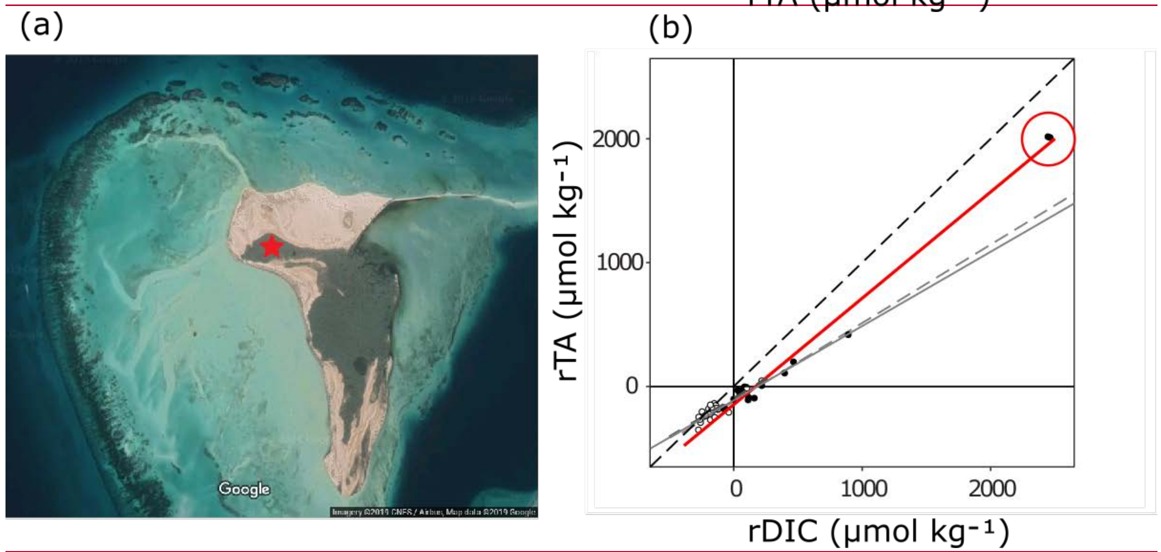

Figure ~~S2~~S3: Panel (a) shows a satellite view of the inland-mangrove stand referred to in the text. The picture was taken using Google Maps satellite view and the red marker indicates the approximate location the two samples that were taken. Panel (b) shows the rTA and rDIC at this mangrove forest site (circled red) against other mangrove forests, in an expanded plot of Figure 8e. The red line indicates the fit of the spatial regression line if this mangrove site is used. All other lines are those displayed in Figure 8e.

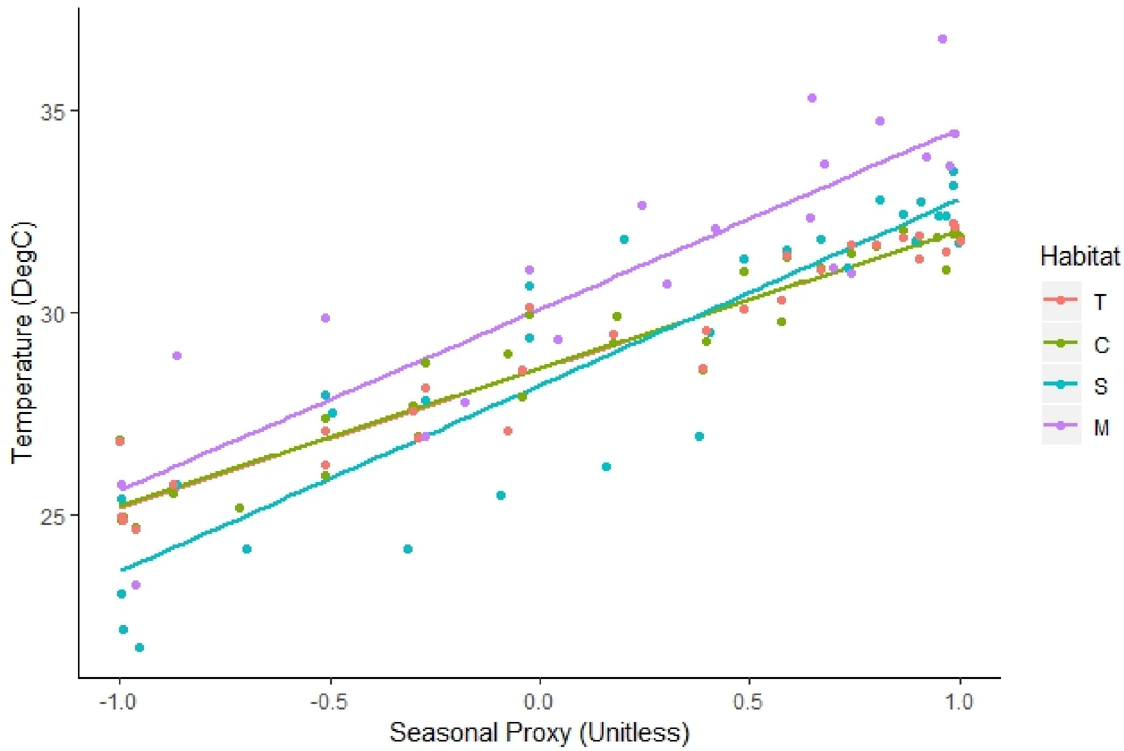

Figure ~~S3~~S4: Interaction plot between the seasonal proxy and habitat type for ~~Temperature~~ temperature for the four coastal time series stations. The four lines indicate linear trends calculates for transition station (T), coral reef station (C), seagrass meadow station (S) and mangrove forest station (M)

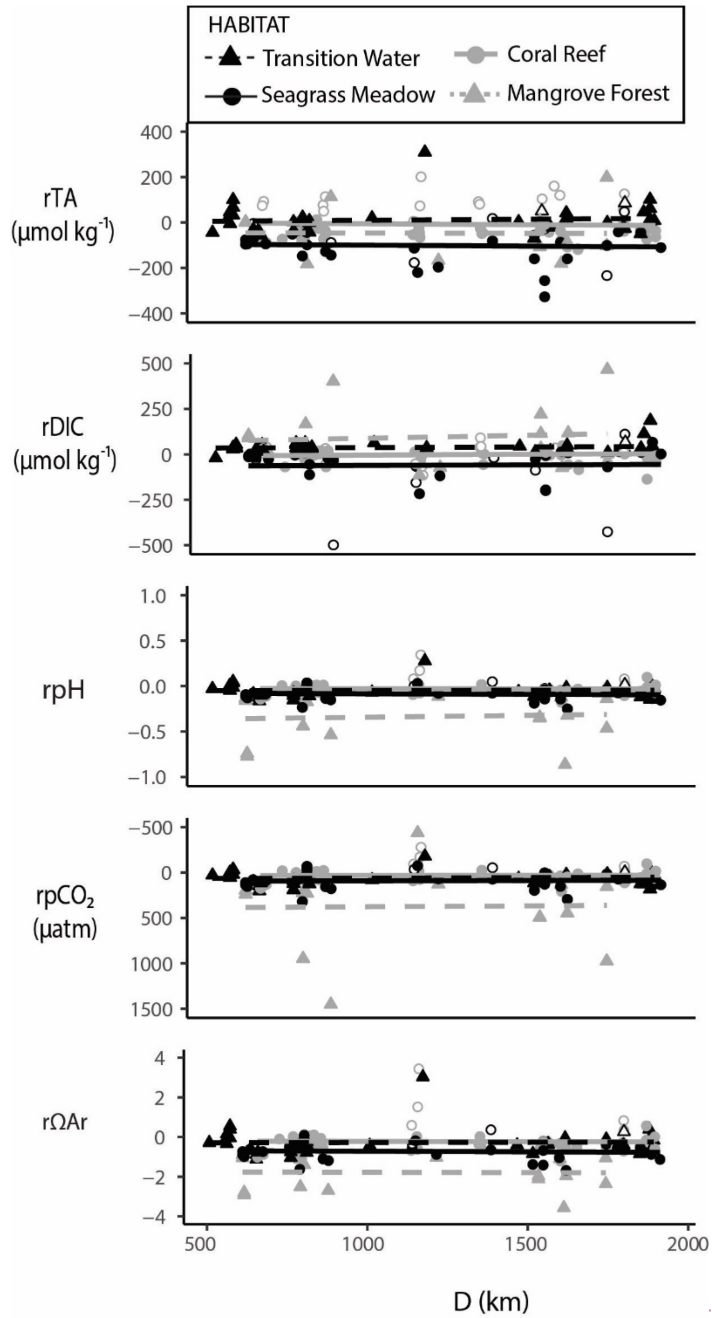
HABITAT
Transition Water
Coral Reef
Seagrass Meadow
Mangrove Forest
rTA (μmol kg-1)
rDIC (μmol kg-1)
rpH
rpCO2 (μatm)
rΩAr
D (km)

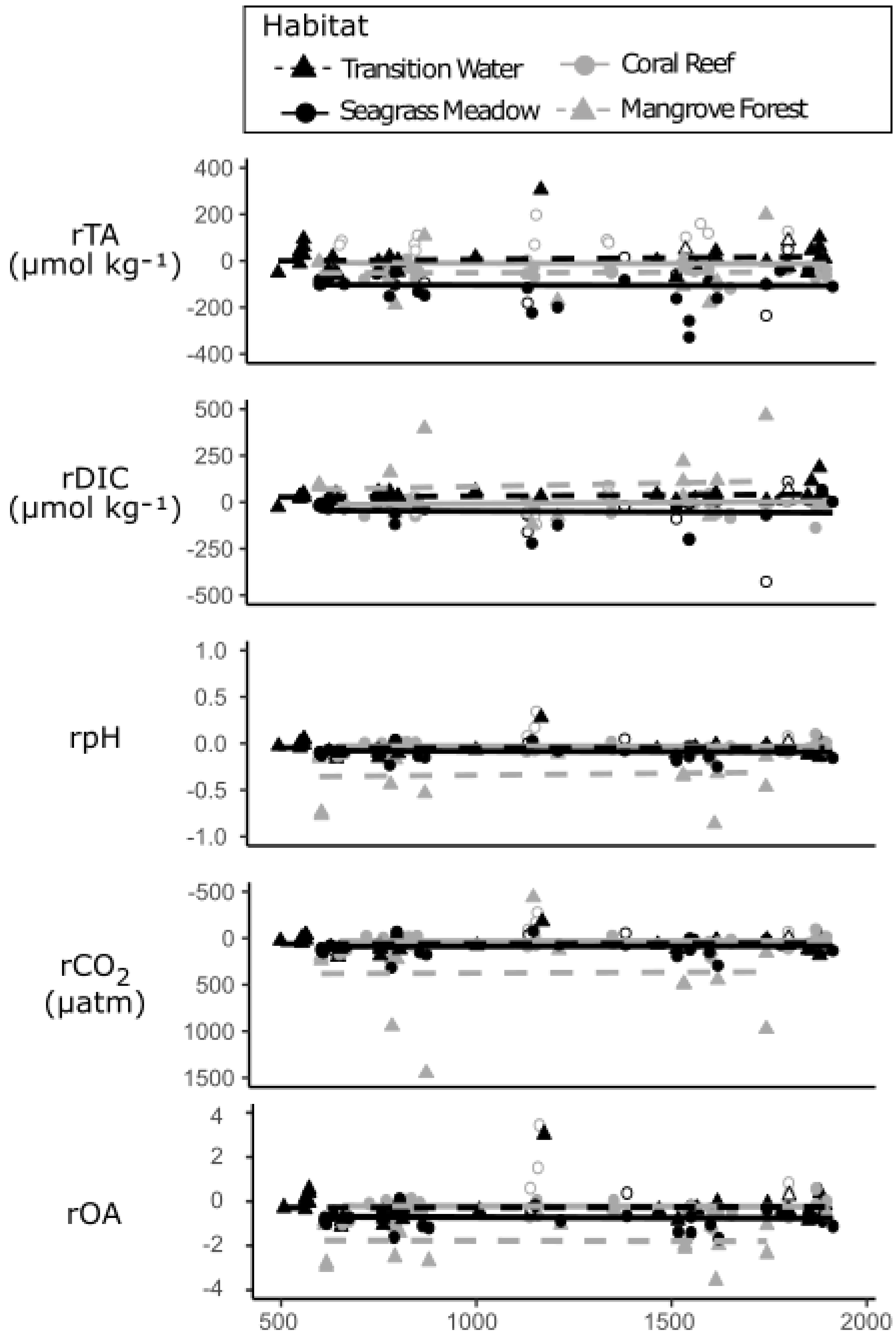

Figure ~~S4~~S5. Residual carbon variables observed in the four coastal habitats are presented against distance along the south-north central axis (D). Linear regressions for all combinations of variables are drawn as lines (although none are significant), with associated statistics reported in Table S3. Note that ~~not all coastal observations are displayed,~~observations from time series stations and the in-land mangroves are excluded. Hollow symbols indicate summer observations.

Table S1. Summary of the observations used in this study. Presented is the cruise code, the source of the data, the month and year in which observations were collected and the number of observations that were collected offshore (O), in transition waters (T) or at coral reefs (C), seagrass meadows (S) and mangrove forests (M).

Cruise	Source	Month	Year	O	T	C	S	M
CSM16	This study	Jan-Apr	2016	13	20	9	11	8
CSM17	This study	Mar	2017	1	5	11	12	9
CCF1	This study	Jan-Mar	2017	0	6	22	5	0
CCF2	This study	Sep-Aug	2017	0	2	17	7	0
CRE	This study	May	2017	1	0	10	2	2
BPC	This study	April	2017	9	6	0	0	0
VOS Pacific Celebes	Hydes et al. (2012)	Nov-Sep	2007-2009	7	1	0	0	0
TARA	Picheral et al. (2014)	Jan	2010	3	0	0	0	0
WHOI	This study	March	2010	53	0	0	0	0
WHOI	This Study	Sep	2011	14	0	0	0	0
STEINER15	Steiner et al. (2018)	Dec-Jan	2015/6	10	0	0	0	0
STEINER18	Steiner et al. (2018)	March	2018	4	1	0	0	0
Total				~~101~~115	~~71~~72	101	69	42

Table S2: Defining statistics for the conservative single-end-member mixing model~~of the normal error for residual carbon variable estimates~~, as calculated from offshore observations

	Residual mean	Residual standard deviation	Lower 99% P.I. bound~~*~~+	Upper 99% P.I. bound~~**~~++	% offshore observations outside the 99% P.I. (excluding/including outliers)
rTA (μmol/kg)	0	~~16.79~~18.37	-~~43.25~~47.31	~~43.25~~47.31	1.~~1/5.9~~0/4.3
rDIC (μmol/kg)	-0.66	~~23.33~~24.59	-~~60.09~~64.00	~~60.09~~62.68	~~2.2/5~~1.9/4.3
rpH	-~~5~~3 x10^{-4}	2.~~69~~61 x10^{-2}	-6.~~97~~76 x10^{-2}	6.~~87~~70 x10^{-2}	~~4.~~3.8/6.~~9~~1
r$p$$CO_2$ (μatm)	-0.~~10~~23	~~30.20~~29.68	-~~77.69~~76.70	~~77.90~~76.24	~~4.~~3.8/7.~~9~~0
rΩ_{Ar}	0.0006	0.~~1879~~1816	-0.~~4833~~4672	0.~~4845~~4684	4.~~3/6.9~~8/7.8

~~*~~+ Residual mean – 2.576*Residual standard deviation
~~**~~++ Residual mean + 2.576*Residual standard deviation

Table S3. ~~By habitat group~~Descriptive statistics for regressions of different variables against D constructed with observations from offshore waters and the four habitat types. Note that observations from time series stations are not included. Pearson's correlation coefficient (r^2), the test statistic (F) and p-value (p) are reported for each individual test.

Table S4. ~~By Habitat descriptive~~Descriptive statistics for carbon variables ~~habitat groups~~ for ~~all~~ coastal observations. Note that observations from time series stations are excluded. The number of observations (n), mean, median, standard deviation, maximum values (max) and minimum value (min) are presented for each habitat group and variable combination.

Table S5. Results from one-way WR-ANOVA and corresponding boot-strapped post-hoc t-tests to identify performed between differences in medians between habitat groups; Offshore (O), Transition waters (T), Coral reefs (C), Seagrass meadows (S) and Mangrove Forests (M). Note that observations from time series stations are excluded. Tests statistics (F for WR-ANOVA and Ψ_hat for post-hoc) and p-values (p) are reported for each individual test.

Table S6. Statistics for regressions of different variables against the seasonal proxy (SP) at the four time series stations. Pearson's correlation coefficient (r^2), the test statistic (F) and p-value (p) are reported for each individual test.

Table S7. Descriptive statistics for studied variables at the four time series stations. The number of observations (n), mean, median, standard deviation, maximum values (max) and minimum value (min) are presented for each time series station and variable combination.

Table S8. Results from one-way WR-ANOVA and corresponding boot-strapped post-hoc t-tests to identify differences in medians between the four time series stations; Transition (T), Coral reef (C), Seagrass meadow (S) and Mangrove Forest (M). Tests statistics (F for WR-ANOVA and Ψ_hat for post-hoc) and p-values (p) are reported for each individual test.

Supplementary R Code: WRS2_post_hoc.R

This code contains 1) the med1way.crit function which is an internal function of the WRS2 package (source: https://github.com/cran/WRS2/blob/master/R/med1way.crit.R) and 2) an adapted version of the mcppb20 function, which is contained in the WRS2 package (source: https://github.com/cran/WRS2/blob/master/R/mcppb20.R), that performs bootstrapped t-tests for differences in medians.